Solar-driven integrated carbon capture and utilization: Coupling CO2 electroreduction toward CO with capture or photovoltaic systems

Solar-driven integrated Carbon Capture and Utilization: Coupling CO_2 electroreduction toward CO with capture or photovoltaic systems

Matteo Agliuzza[a,b,§], Alessio Mezza[a,b,§], Adriano Sacco[a,*]

[a] *Center for Sustainable Future Technologies @Polito, Istituto Italiano di Tecnologia, Corso Trento 21, 10129 Torino, Italy*

[b] *Applied Science and Technology Department, Politecnico di Torino, Corso Duca degli Abruzzi 24, 10129 Torino, Italy*

[*] Corresponding author: e-mail adriano.sacco@iit.it, Tel. +39 011 5091912, Fax. +39 011 5091901.

[§] These authors contributed equally to this work.

Abstract

Electrochemical processes have emerged as intriguing strategies for both CO_2 capture and valorization, which are needed to combat global warming and climate change. Among other advantages over competing technologies, electrochemical systems can be powered by renewable sources, including solar energy.
This review aims at collecting and analyzing the main works proposed in the literature that study the coupling of electrochemical reactors for the conversion of CO_2 into carbon monoxide with 1) electrochemical capture systems or 2) solar cells to power them. In addition to the critical analysis of these articles, a brief discussion of future research directions in this field is proposed.

Keywords: CO_2 capture and conversion; solar cells; carbon monoxide; electrochemistry.

1. Introduction

As the 21st century progresses, the problem of global warming becomes more and more pressing on our planet. This phenomenon is represented by the average rise in terrestrial temperatures (and a corresponding reduction of rainfall), leading to an increase, both in frequency and intensity, of phenomena such as hurricanes, fires and floods as well as the growth of sea level caused by the melting of glaciers and the desertification of places. This causes problem for biodiversity, due to abnormal migrations, food shortages and hard living conditions [1]. It can be undoubtedly affirmed that this situation has been largely caused by the human activities [2]. Since the industrial revolution, large amounts of greenhouse gases (GHGs) have been emitted in the atmosphere, substantially contributing to the rise in temperatures and to the problems mentioned above. Among the GHGs, carbon dioxide (CO_2) is the one with the largest concentration in the environment and the longest residence time, thus representing the most impacting climate-altering substance [3]. Moreover, its concentration had the greatest increase from the pre-industrial age up to now. To face the global warming issues, different policies have been established in the recent years. In 2015, the COP21 was held and the Paris agreement was signed. With this agreement, the goal was to keep the temperature increase (compared to the pre-industrial era) to a maximum of 2 °C [4]. In 2020, the EU published the 'European Green Deal', which sets the goal, within 2030, of reducing emissions by 55% (compared to 1990) [5]. This target was revised in 2021 following COP26 in Glasgow, with the main objective to keep the temperature increase within 1.5 °C [6].
To reduce the CO_2 emissions and its accumulation in the atmosphere, carbon capture and utilization (CCU) technologies have been proposed as effective solutions [7-10]. Indeed, some CCU pilot plants were already been established all over the world [11-13] and additional ones are planned to be built in the next years [14-16], witnessing the disruptive potential that these technologies can offer. In particular, different strategies can be adopted for carbon capture and separation from flue gas (in order to have more details on this class of

technologies, the reader is invited to have a look on other recently published reviews [17-19]). Among them, the one which is widely adopted is the absorption process using chemical solvents like amines [20]. However, amines are toxic substances, and the energetic costs for their regeneration is not negligible [21, 22]. For what concerns the CO_2 conversion, also in this case different technologies have been proposed in the literature, including, biochemical, enzymatic, photochemical, electrochemical and thermochemical routes [23-25]. The latter represent the most employed one, mainly due to the high efficiency and the capability of obtain large variety of output molecules [26], even though relatively high temperatures are needed to carry out the conversion [27, 28].

In this framework, electrochemical processes demonstrated to be intriguing strategies for both CO_2 capture [29-31] and valorization [32-34]. Indeed, electrochemical routes can guarantee many advantages over the remaining technologies: the processes are repeatable and controllable and can be carried out at mild conditions; it is possible to use green chemicals as reagent and/or supporting electrolytes; the employed reactors are easily up-scalable and compact [35]. Moreover, being both capture and valorization electrochemically-based, the coupling of the two processes become easier, thus providing additional advantages, such as reduced costs for CO_2 transport and potential downstream apparatuses [36, 37]. Finally, another fascinating characteristic is the possibility for electrochemical systems to be powered by renewable sources, in particular by the Sun [38, 39]. This can be seen as a sustainable route for store the excess solar energy that is not put in the electric grid [40], globally allowing a carbon neutral (or even negative) path [41].

Among the different products obtainable from the electrochemical CO_2 reduction reaction (CO_2RR), techno-economic analyses showed that carbon monoxide (CO) is the one with the highest profitability [42, 43]. In fact, CO can be easily produced at relatively low overpotentials through a 2 electron-reduction pathway [44], and it is widely employed in the chemical industry, representing the most significant and versatile C1-building block [45]. As an example, it used at large industrial scales in the Monsanto/Cativa acetic acid synthesis [46] and, together with hydrogen (H_2) forms then synthesis gas (syngas) [47], which is exploited in the Fischer-Tropsch synthesis of hydrocarbons [48], and in internal combustion engines [49]. This represent a plus for the electrochemical CO_2RR (eCO_2RR) to CO, since usually the hydrogen evolution reaction (HER) is seen as a competing reaction in water-based electrolytes, while in this case CO_2RR and HER can be carried out simultaneously to obtain syngas with tunable composition [50].

Based on all these premises, it is clear that an all-electrochemical system, consisting of the coupling of (i) a CO_2 separation and capture module and (ii) a conversion module, powered by solar energy, is of crucial interest in order to face the global warming issue. To this end, the aim of this review is to critically analyze the solutions proposed in the literature, which, to the best of our knowledge, do not include a single integrated system. Therefore, after a brief introduction on eCO_2RR in Section 2, the coupled capture-conversion approaches are reviewed in Section 3, while in Section 4 the solar-driven conversion systems are discussed. Finally, Section 5 will present the future perspectives, suggesting some strategies that are not yet explored by the scientific community.

2. Electrochemical CO_2 reduction reaction

The eCO_2RR is a mechanism for which carbon dioxide is converted in value-added molecules, usually in aqueous electrolytes. Thanks to Proton-Coupled Electron multi-Transfer (PCET), in fact, multi-electron transfer occurs between the electrode and the CO_2 molecules (which can be dissolved in the electrolyte or in a gaseous stream), thus reducing them. This electron transfer, enabling the reduction of the CO_2, occurs at the cathode, while protons (H^+) and electrons are provided by an oxidation reaction occurring at the anode (such as the oxygen evolution reaction, OER). Relations (1-4) summarize the main reactions occurring at the anodic (1 and 2) and cathodic (3 and 4) compartments of the electrochemical cell for the CO production (3) and HER (4).

$$2H_2O \rightarrow 2H^+ + 2OH^- \quad (1)$$

$$2OH^- \rightarrow H_2O + 1/2\,O_2 + 2e^- \quad (2)$$

$$CO_2 + 2H^+ + 2e^- \rightarrow CO + H_2O \quad (3)$$

$$2H^+ + 2e^- \rightarrow H_2 \quad (4)$$

The latter is a competitive reaction with respect to CO_2RR (relation 3), and often reduces the selectivity toward the carbon products. In this framework, an important parameter for quantifying the selectivity of the device toward the different products of the electroreduction is the Faradaic Efficiency (FE). This parameter describes the efficiency of the electric charge to participate to a particular electrochemical reaction (for example, formation of CO), and is calculated as the total charge involved in the product formation over the total charge passing through the system:

$$FE = \frac{\chi n F}{Q} \quad (5)$$

where χ is the number of moles of the product of interest, n the number of electrons transferred per mole of product, F the Faradaic constant, and Q the total charge flowing through the electrodes. Unless otherwise specified, all the FE values reported in this review refer to CO.

The CO_2RR is favored by the presence of a catalyst, which is the key component for the selectivity of the final product. The catalytic activity towards a specific product, in fact, is governed by the binding strength towards certain intermediates, and the ability of binding CO_2 molecules on the vacant coordination sites on the reduced catalyst surface [51]. It is well demonstrated in literature that the final product formation is determined by carbon-bound intermediates: for the conversion of CO_2 in CO, the reaction pathway is determined by the initial formation of adsorbed hydrogenated reaction intermediates, such as *COOH or *OCHO [52]. For further details, interesting *in-situ* techniques have been exploited to study the process of adsorbed intermediate formation and the catalytic reaction mechanisms [53].

While the catalyst governs the reaction kinetics and the final product selectivity, the overall performance of the electrochemical cell is influenced on a series of factors: type of electrolyte and molar concentration [54], pH [55-57], pressure [58], temperature [59] and eventual poisoning of the catalyst [60-62]. Lastly, there exist different electrolyzer designs (as shown in Figure 1), which lead to different operational conditions and electrochemical performance. The single-type cell (Figure 1a) is the simplest configuration, in which both anode and cathode are immersed in the same electrolyte without separation. In the H-type cell (Figure 1b) an ion exchange membrane divides the cathodic and anodic compartments: the membrane adds an ohmic loss, but it allows for a physical separation between the electrodes, such that liquid products do not cross-over from catholyte to anolyte. In the flow cell (Figure 1c), Gas Diffusion Layers (GDLs) allows the transport of gaseous CO_2 molecules to the electrode, thus reducing mass transport limitations. Lastly, in the zero-gap cell (Figure 1d), no distance is present between the catalysts (both cathodic and anodic ones) and the membrane, thus further improving the mass transport. For more detailed information regarding the different cell types, some reviews are proposed to the reader taken from literature [63-65].

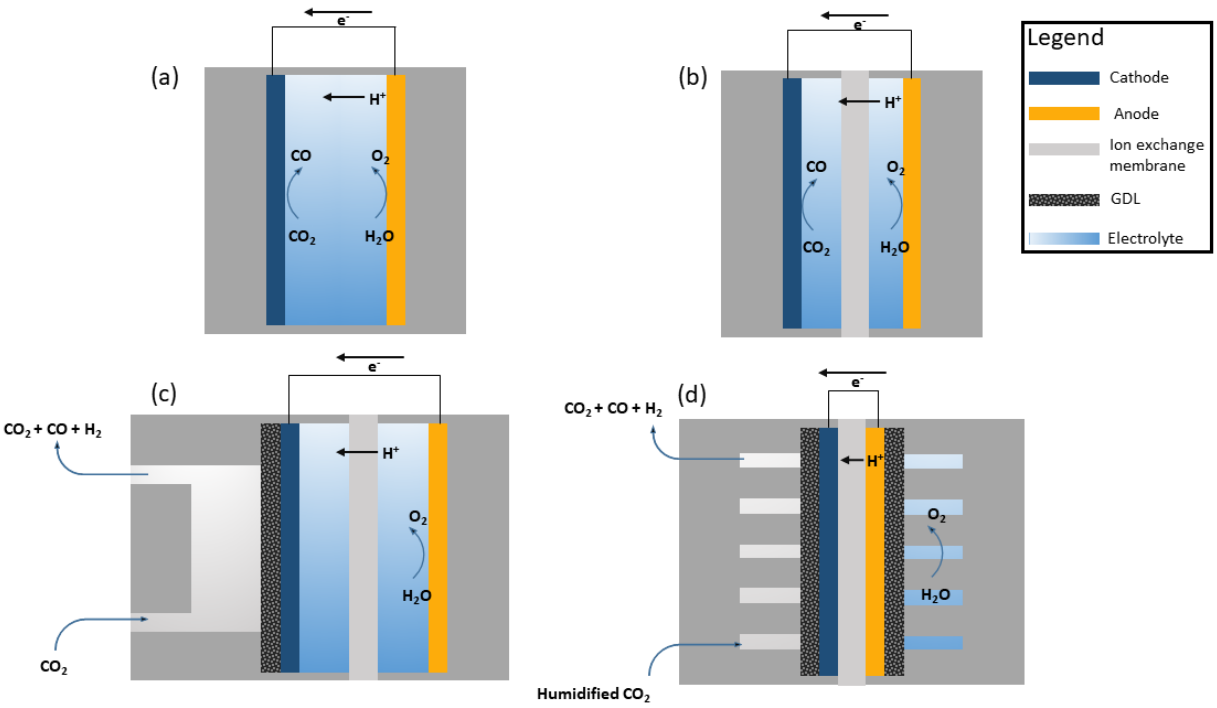

Figure 1 *Schematic representation of typical electrochemical reactors for CO_2 reduction: a) single cell, b) H-type cell, c) flow cell, d) zero-gap cell.*

3. Electrochemical carbon capture and valorization systems

Techniques for the electrochemical conversion of CO_2 have evolved very rapidly in last years. In this framework, there is a growing interest in looking for suitable carbon capture methods that separate the CO_2 from flue gases, and convert it into added-value chemicals. Among the many capture technologies already studied [66, 67], a deep investigation is needed to understand which are actually appropriate to match with a CO_2RR reactor in terms of optimal working condition. In this framework, it is important to highlight the difference between coupled and integrated systems. In a coupled system (Figure 2a), the separation of gaseous CO_2 from the flue gas occurs in a dedicated device whose outlet is sent to the reactor responsible for the electrochemical conversion. On the other hand, an integrated system (Figure 2b) is able to capture and convert CO_2 in a single device using a novel technique that receive as inlet a flue gas and delivers as outlet the eCO2RR products. In the next paragraphs some electrochemical capture technologies that could potentially be coupled/integrated with a typical CO_2RR reactor [68] are presented.

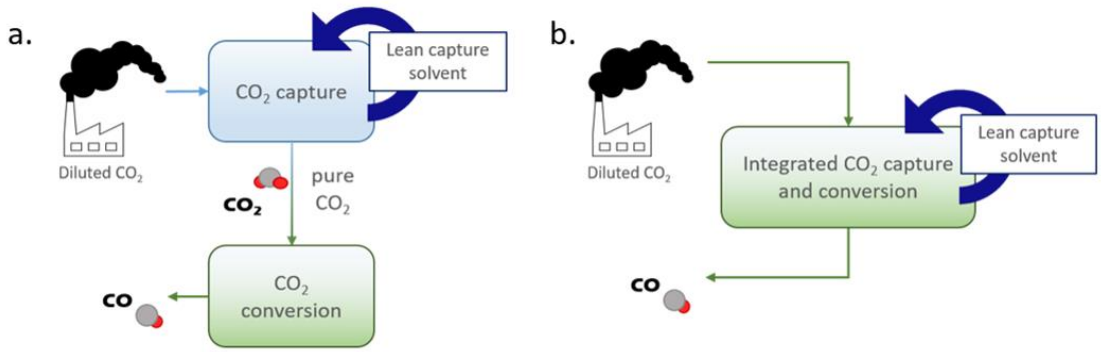

Figure 2 *Schematic illustration for a CCU system with (a) coupled capture and conversion and (b) integrated capture and conversion.*

3.1 Coupled systems

Electrochemical CO_2 capture technologies from point sources have attracted strong interest, since they eliminate the need for thermal energy necessary for the CO_2 stripping from the sorbent solution that is present in amine-based capture methods [69]. The utilization of a pH-swing for the CO_2 absorption and release, implemented by ions exchange membranes and electrodialysis of alkaline carbonate solution, is reported in several works [29, 70]. Sequences of bipolar, cation and/or anion exchange membranes are used to create a pH difference between the compartments of the electrochemical cell, allowing for release and regeneration of the sorbent solution. This system can reach high CO_2 removal rate increasing the current density by keeping a high voltage. However, above 1.23 V vs Reversible Hydrogen Energy (RHE), water splitting occurs producing H_2 and O_2, thus reducing the global efficiency. Mezza *et al.* [36] showed that it is possible to couple such a system (Figure 3) with an eCO_2RR cell. CO_2 was successfully filtered from the flue gas through wet scrubbing in NaOH and released into a conversion reactor based on a nanostructured ZnO catalyst on gas diffusion electrode [48] that converted it into CO. Xiang *et al.* [71] reported a proof-of-concept of an electrochemical system exploiting a bipolar membrane electrodialysis cell and a CO_2 reduction cell to extract and convert CO_2 from ocean water. In this last work, catholyte and anolyte contain a reversible redox-couple solution, hence avoiding the water splitting reactions (Figure 4) and increasing the extraction efficiency.

Other techniques are currently being developed [67, 72] to perform CO_2 capture at low energy and they could potentially be useful to build an efficient electrochemical platform. The pH-swing can be enabled by proton carriers undergoing redox reactions whose energy requirement is smaller with respect to electrodialysis mechanisms mentioned above. CO_2 is captured forming an alkaline solution obtained via the reduction of the redox molecule, then it is released through acidification by re-oxidation. This idea has been implemented by Xie *et al.* [73] using riboflavin 5'-monophosphate sodium salt hydrate, and by Kwabi *et al.* [74] using sodium 3,30-(phenazine-2,3-diylbis(oxy))bis(propane-1-sulfonate), as redox proton carriers, respectively. The first one allowed a very low energy dispersion (9.8 kJ per mole of CO_2 desorbed), in addition to have a biological low cost redox-active species. Although these systems are potentially suitable to have eco-friendly closed carbon cycle, they have several practical problems. Firstly, they are vulnerable to oxidizing gases and O_2 is a component of flue gasses. Moreover, the poor cycle performance and the very low release rate make these technologies still underdeveloped to be used in an operative CO_2 capture and conversion system.

In addition to the intrinsic problems of these technologies, several practical issues occur when the capture and the conversion modules are coupled. For instance, the release of CO_2 from an aqueous solution does not ensure a good, pressurized carbon dioxide stream able to feed the CO_2RR reactor. Moreover contamination of other gasses arising from the capture cell (e.g. O_2) strongly affects the FE for CO [75].

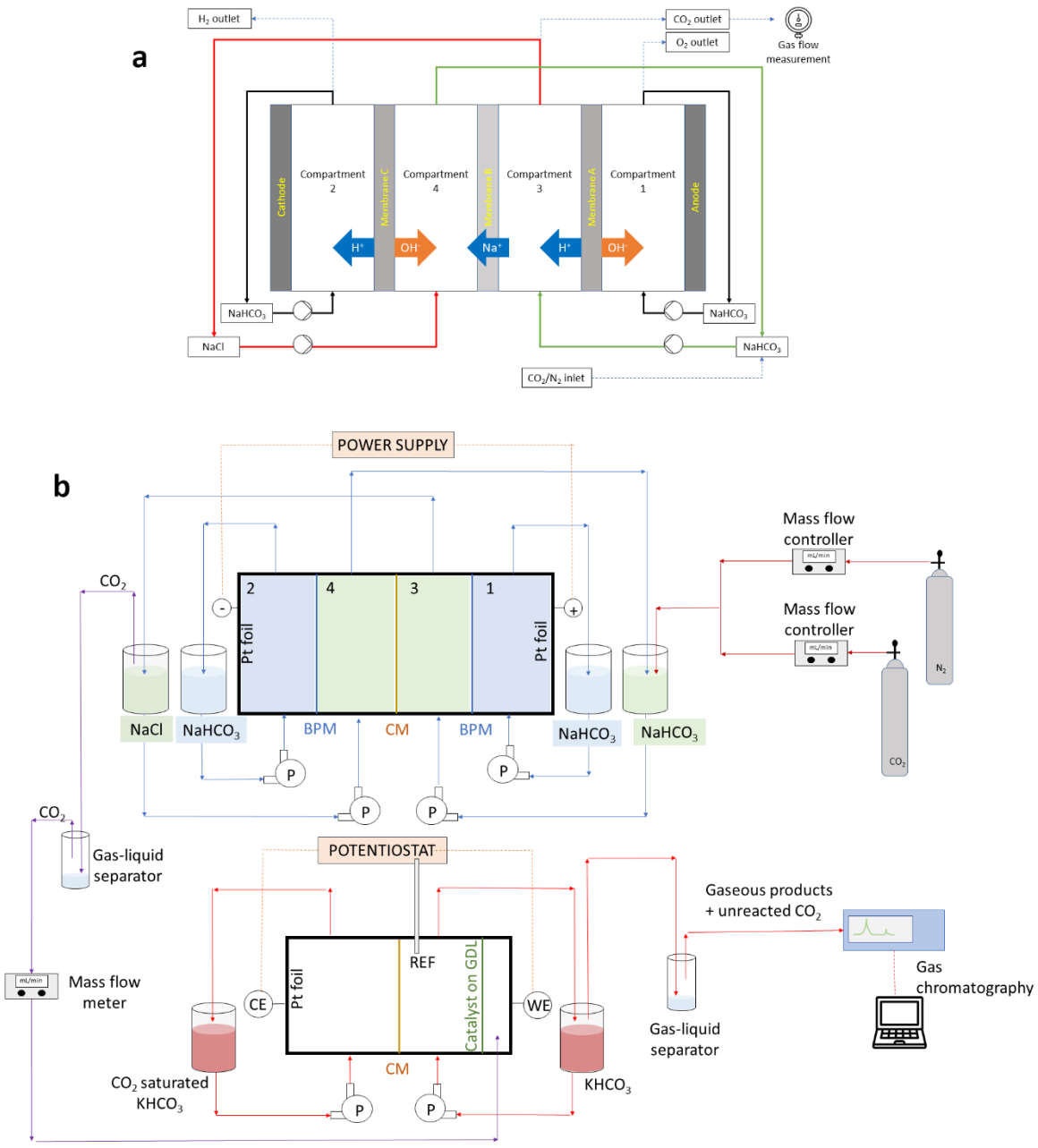

Figure 3 *CO_2 capture and conversion reported by Mezza et al. a) Electrodialysis cell made by two bipolar membranes and two cationic exchange membranes. b) Schematic representation of the process flow including CO_2 capture by wet scrubbing in sodium hydroxide, CO_2 recovery in the electrodialysis cell and conversion into CO in CO_2RR reactor with ZnO on gas diffusion layer. Reprinted with permission from [36].*

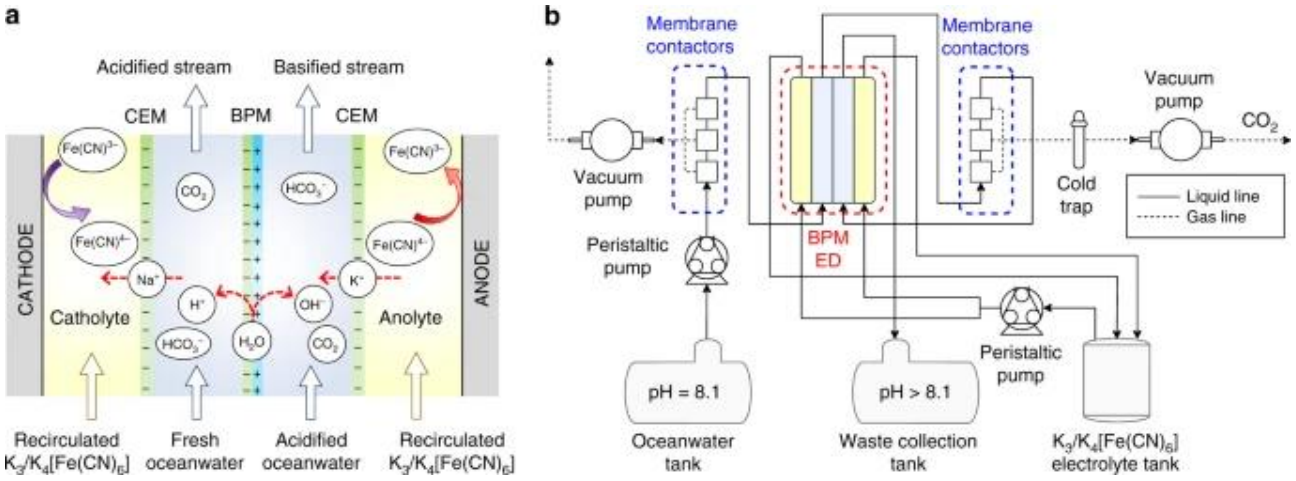

Figure 4 *CO_2 recovery from oceanwater reported by Xiang et al. a) Electrodialysis cell made by a bipolar membrane and two cationic exchange membranes. The redox couple $Fe(CN)^{3-}/Fe(CN)^{4-}$ is used to avoid HER and OER at cathode and anode. b) Schematic representation of the process flow to get a CO_2 stream from ocean water to feed the conversion reactor. Reprinted with permission from [71].*

3.2 Integrated systems

The integration of carbon capture and utilization (ICCU) permits to solve some of the problems mentioned above. As already shown in Figure 2b, the idea consists in combining the processes employed in CCU using the captured media as an electrolyte inside the electrochemical reactor for the valorization. One way is to release gaseous CO_2 from the capture media directly near the electrocatalyst responsible for the conversion. The other road is to avoid the energy-intensive CO_2 desorption from the sorbent agent, performing the electroreduction directly on CO_2-loaded capture agents. This implies that the reactor is always fed by high concentration of CO_2, decreasing the mass transfer limitation present in CO_2RR performed in classic batch cell due to the poor solubility of CO_2 in aqueous solutions (34 mM). This is a critical step for the Faradaic efficiency of the conversion [76].

For all these reasons, especially if powered by renewable energy, ICCU makes the whole process capture-valorisation more economically advantageous [77, 78]. However it has been calculated that, from an energy perspective, an integrated conversion system must work below 1000 kJ/mol_{CO2} to guarantee a minimum energetic benefit of 44% with respect systems performing sequential capture and conversion present in the state-of-the-art [79].

In the following, the most promising methods for electrochemical ICCU are reported, focusing on CO as product.

3.2.1 Amine-based integration

Nowadays, most part of commercial capture systems exploit amine-based technologies since they are well known for the reversible reactions with CO_2 [69]. The first trials to integrate capture with conversion used an amine compounds as electrolyte for the electrochemical conversion of CO_2 [80-82]. The most utilized capture solvents for CO_2 are monoethanolamine (MEA) [83] and of 2-amino-2-metyl-1-propanol (AMP) [84], that are thermally regenerable. CO_2 reacts with these substances forming carbamate species [85].

Pérez-Gallent *et al.* [82] carried out the CO_2 electroreduction in a mixture of AMP and propylene carbonate (PC). The solvent with the carbamate-species is sent to the cathodic compartment of a CO_2RR reactor. CO_2 is desorbed near the electrode as a result of the equilibrium reactions (8) for the carbamate formation:

$$2\mathrm{RNH_2} + \mathrm{CO_2} \rightleftarrows \mathrm{RNHCOO^-} + \mathrm{RNH_3^+} \qquad (6)$$

The temperature is kept around 75 °C in order to reverse (6) and promote the release of CO_2, which is then electrochemically reduced. This temperature is easily reached exploiting the Ohmic losses, that usually are a

drawback, in standard industrial electrolyzer [86]. This procedure is the one denoted as route (a) in Figure 5. This system, working in a flow cell with AMP 1 M in PC with Au as catalyst at 75 °C, reached a FE of 45% for CO with cathode potential of -1.6 V vs Ag/AgCl and 15 mA/cm^2.

Except for this example, the main road followed by the research focused on the integration through amine-based processes, is based on the direct electro-reduction (route (b) in Figure 5) of CO_2-loaded adduct (i.e. $RNHCOO^-$) obtained by purging the amine compounds with CO_2, avoiding high temperature for the release of gaseous CO_2 in the cathodic chamber [87-90]. This permits to have gaseous products (e.g. CO and H_2) that are not diluted with unreacted CO_2. Hence, amines and catalyst has started to be studied in recent works to make them suitable for the reduction of carbamates at high FEs. Abdinejad *et al.* [91] studied the electrocatalytic activities of some commercial amine compounds on Cu electrodes. In particular three different compounds has been tested: MEA [83], that form carbamates salts in viscous form, ethylenediamine (EDA) [92] and decylamine (DCA) [93], forming white solid carbamate salts. As reported in Figure 6, EDA-CO_2 provides the highest current density for Cu electrodes (in Figure 6b the peak pair of Cu oxidation can be observed). In particular, it has been performed a chronoamperometry at -0.78 V vs RHE with a current density of 18 mA/cm^2 furnishing a FE for CO of 58%.

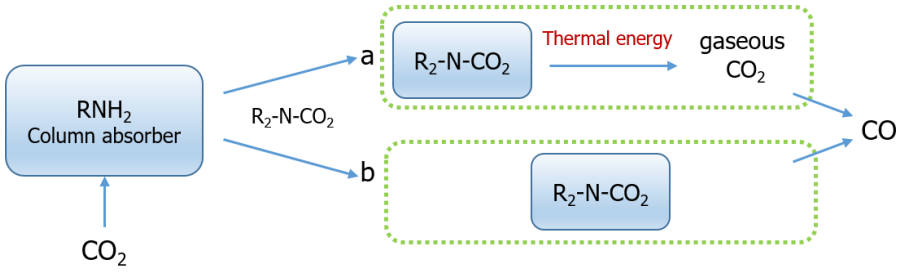

Figure 5 *The two roads to implement ICCU through ammine-based processes: a) gaseous CO_2 is released from the CO_2-rich solvent in proximity of the cathodic catalyst in order to be converted into CO; b) the electroreduction is directly performed on the CO_2-loaded adduct (i.e. carbamate).*

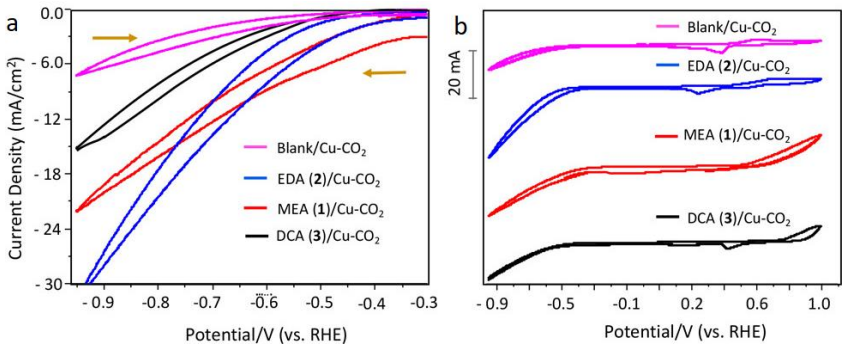

Figure 6 *Cyclic voltammetry of different CO_2-loaded commercial amine compounds on Cu electrodes in electrochemical H-cell: a) focus on the cathodic potentials, b) full potential range. Reprinted with permission from [91].*

The direct electrolysis of carbamates offers an advantageous approach; however, FEs are poorer than classical systems for eCO_2RR. Lee *et al.* [94], using MEA as electrolyte, got a FE of 5% toward CO with an Ag electrocatalyst, a good and well known material for CO_2 electroreduction. They suggested that this is due to the inefficiency of electron transfer between the electrode and the carbamate molecule; therefore, they deeply investigated the charge transfer between the surface and species in the electrochemical double layer (EDL). The EDL is formed by ethanolammonium and carbamate (since carbamate ions are anions they could be repelled by the cathode surface). The introduction of properly sized electrolyte ions can disrupt the undesired charge-blocking layer, suppressing the hydrogen evolution by minimizing surface coverage of protonated amines and achieving the desired electron transfer to carbamate [79]. Adding KCl (2 M) in 30 wt% aqueous MEA solution, the FE_{CO} increased up to 72% at 50 mA/cm^2 and -0.8 V vs RHE. However, this result has been obtained still heating the catholyte at 60 °C, in order to make the N-C bond weaker and promote the carbamate

electroreduction. It should be mentioned that including alkali cations destabilizes the formation of carbamate, affecting the absorption capacity of MEA [95], therefore a trade-off is necessary to favour the carbamate conversion at the lowest possible cost on CO_2 capture.

3.2.2 CO_2 electro-reduction from (bi)carbonate aqueous solution

Most recent works on CO_2RR reached good current densities and high FEs, especially toward CO, using CO_2-fed systems exploiting Gas Diffusion Electrodes (GDEs) [96]. Although there are important advantages in delivering liquid rather than gas to the CO_2RR reactor, the very low solubility of CO_2 in aqueous solutions makes fundamental the utilisation of the gas feed.
However, imaging to have only liquid feed containing bicarbonate, a bipolar membrane (BPM) delivering H^+ to the cathode makes the HCO_3^- reacting and generating gaseous CO_2 [97] (reactions 7 and 8) that may be then available for the electro-reduction without any external CO_2 supply [98, 99].

$$H^+ + {CO_3}^{2-} \rightarrow {HCO_3}^- \quad (7)$$

$$H^+ + {HCO_3}^- \rightarrow CO_2 + H_2O \quad (8)$$

A common system to capture CO_2 is by reaction with an alkali hydroxide solution into HCO_3^- [100]: therefore it would be possible to use bicarbonate derived from capture as carbon reservoir for the carbon dioxide valorisation. In addition, since the electroreduction of CO_2 into CO follows the reaction (9), derived from the combination of reactions (1) and (3), the OH^- formed may be used to regenerate the hydroxide sorbent solution, providing a closed circle able to capture and convert CO_2.

$$CO_2 + H_2O + 2e^- \rightarrow CO + 2OH^- \quad (9)$$

Gaseous CO_2 is formed at the interface of the BPM where protons are delivered. Hence, since the catalyst has to be in contact with the membrane in order to suppress the HER, Membrane Electrode Assembly configuration is necessary. This configuration follows a different arrangement of the typical CO_2RR reactors elements, as shown in Figure 7 [101, 102].

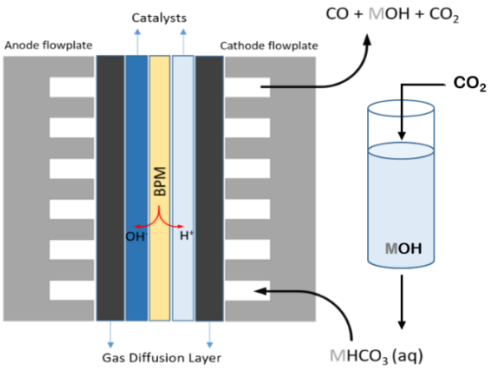

Figure 7 *Schematic representation of a fuel cell-like electrolyzer for CO_2RR from bicarbonate for a closed carbon circle. M is a general alkali cation.*

It has been shown that the electrochemically active specie is not the (bi)carbonate, but the gaseous CO_2 released from that one [98]. The conversion from bicarbonate to CO is enabled by an acidic zone near the membrane interface activating the CO_2 release and by a basic region at the catalyst arisen from the generation of OH^- from the eCO_2RR. This whole process is based on a different mechanism with respect the most explored systems exploiting amines, for which research tends to explore the road of the direct CO_2-loaded adduct, e.g. carbamate.
Li *et al*. [99] used the set-up reported in Figure 7 exploiting Ag nano-structured cathodic electrocatalyst and Ni foam as the anode. They compared the performance of the conversion with pure and capture-generated

K_2CO_3. Firstly, as shown in Figure 8, the FE_{CO} increases with increasing the concentration of KOH of the sorbent solution: this leads to augment the capture-generated K_2CO_3, hence the carbon source. Moreover, there is a slight improvement in FE with respect the case of pure K_2CO_3 electrolyte, probably due to the fact that purging CO_2 in the sorbent solution, not only increases the carbonate concentration, but it generates also a small amount of dissolved CO_2, giving an additional contribution to the reservoir of reactant.

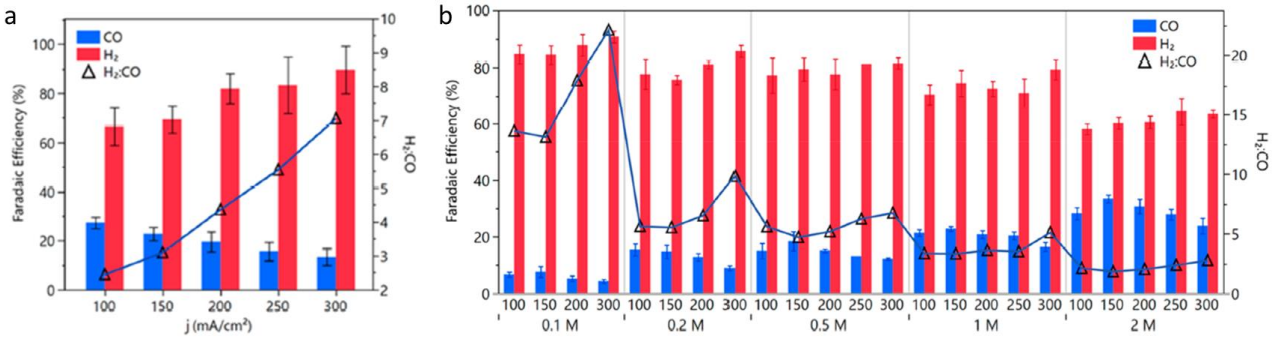

Figure 8 *FE_{CO} obtained by Li et al. In (a) the experiments have been conducted with 1 M K_2CO_3 with nitrogen purging to avoid dissolved CO_2. In (b), the experiments have been conducted with different concentrations of KOH purged with CO_2 to simulate products generated by the capture solution. Reprinted with permission from [99].*

Li *et al*. [98] carried out similar experiments using pure $KHCO_3$ as catholyte supposing to be the product of CO_2 capture from KOH and investigated the role of the BPM and the effect of the concentration of the electrolyte. Using a 4 cm^2 membrane electrode assembly with nickel foam anode and silver nanoparticles at the cathode, they confirmed that increasing [$KHCO_3$] brings an improvement of the FE_{CO} (Figure 9b), in agreement with Li *et al.* [99] However, they observed very small differences comparing the case of CO_2-saturated and N_2-saturated $KHCO_3$ electrolytes. On the other hand, fixing the current at 20 mA/cm^2, at low electrolyte concentration, the FE_{CO} in CO_2-saturated solution is doubled, while the difference is negligible for 2.5 M and 3 M. Data reported in Figure 9c explains how much the employment of a BPM in such a system is fundamental. In the case of an Anion Exchange Membrane (AEM) the build-up of OH^- would deplete HCO_3^- forming CO_3^{2-}. Therefore, the high concentration of protons (lowering the pH) delivered by the BPM facilitates the conversion of CO_3^{2-} in HCO_3^-, that is then converted into CO_2 through acid/base process. BPM is able to boost the formation rate of the carbon dioxide, providing a higher concentration of CO_2 at the outlet, and consequently an important gain in FE_{CO}.

Although these works furnish important information for a simple integration of carbon capture and valorization, classic gas-fed electrolyzer reaches higher current density and FE. Therefore, it is very important to better understand how the performance may be improved. Fink *et al*. [103] studied how the alkali-metal cation can influence the selectivity of the conversion of HCO_3^- in order to select the optimal bicarbonate electrolyte that may be used for ICCU. The amount of CO_2 generated and available at the catalyst results to be controlled only by the H^+ flux from the BPM and mass transport of HCO_3^-, not by the identity of the cation. On the other hand, the selectivity for the CO increases with the cationic radius. This is coherent with what has been already seen in the standard electrochemical reduction of CO_2 [104]. In all the works mentioned so far, at the anodic side of the fuel cell-like electrolyzer, KOH is used as electrolyte, hence without the need of the gas diffusion layer. In Zhang *et al.* [105], humidified H_2 gas flows on the anode side reacts with a gas diffusion electrode made by Pt on carbon black. Therefore, using hydrogen oxidation reaction (HOR) instead of OER as source of protons, for a constant current of 500 mA/cm^2, the total cell potential is below 2.3 V, which is a very small value for such kind of electrolyzer: the drawback is that the FE_{CO} are quite low. Moreover, a microfluidic buffer layer between the silver cathode and the membrane has to be employed: this permits to suppress the HER in favour of the CO_2RR. Also, since H_2 gas must be produced by water electrolysis, the advantage gained by the small cell voltage must be evaluated with respect the power needed to produce hydrogen.

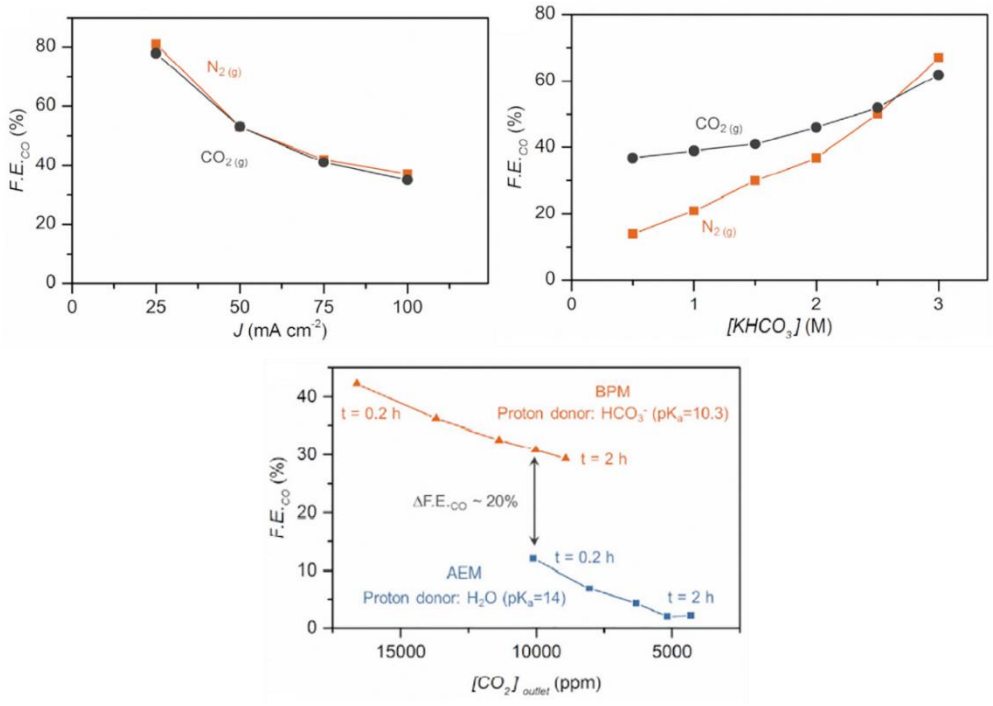

Figure 9 *a) FE_{CO} for CO_2 and N_2-saturated as a function of the current applied. b) FE_{CO} for CO_2 and N_2-saturated as a function of the electrolyte concentration at 20 mA/cm^2. c) CO_2 concentration at the outlet of the cell and the corresponding FE_{CO} during a time working of 2 hours. Reprinted with permission from [98].*

3.2.3 CO_2 capture and conversion with ionic liquids

Ionic liquids (ILs) are currently a promising solution to substitute amines as a CO_2 capture media [89, 106-108]. At ambient conditions, the strong ion-ion interactions provide a very low evaporation. Also, they are characterized by high thermal stability and large electrochemical window. ILs are inflammable and non-volatile, which make them more environmentally friendly than other solvent such as amines. Furthermore, important chemical and physical properties are tunable by choosing the proper cation or anion part with certain functional group, such that a task specific ionic liquid (TSILs) can be synthesized [109]. Ionic liquids are also emerging as electrolyte in the electrochemical conversion of CO_2, since they are able to promote the production of useful chemical feedstock [110, 111].

CO_2 electroreduction has been studied for several years and, although great advances have been made, the intrinsic limit due to the low concentration of dissolved CO_2 in aqueous electrolyte makes difficult to keep high current density without a further gas fed into the reactor. Rosen *et al.* [112] firstly reported a very selective electroreduction of CO_2 into CO using Ag cathode in a mixed ionic liquid water solvent system. In particular, they obtained a lower overpotential with respect the one that is usually obtained in absence of the ionic liquid. In addition, it has been shown that IL suppress the HER, since it limits the diffusion of H^+ to the catalytic sites [113, 114]. Given this information, there is a concrete possibility to exploit ionic liquids to develop systems where the electrocatalytic reduction is carried out within the capture media.

Tanner *et al.* [115] studied the influence of the electrode material, cation and anion of IL on the peak potential of CO_2 reduction using IL-based electrolyte. Figure 10 highlights the main results of the work. The influence of electrode material on the electroreduction of CO_2 in [Bmim][NTf_2] [116] has been explored and results are reported in Figure 10a. In the cyclic voltammetry of glassy carbon and platinum, there is no peak corresponding to CO_2 reduction, while with gold and silver electrodes the current density peaks associated to the one-electron reduction of CO_2 are evident. Therefore, the enhanced reduction of CO_2 in ionic liquids previously observed [112] is dependent on the material of the electrode. In particular, silver is able to considerably catalyse the process. Figure 10b and 10c are significant for what concerns the tunability of the chemical properties of ILs. It has been shown that varying the anionic and/or cation part the potential of the reductive wave shifts; in addition, the current density relative to the peak could be increased. However, the differences observed on the

peak current density for different anions/cations are relatively small with respect the influence given by the electrode material. As observed by Tanner *et al.* [115], although [Bmim][FAP] [117] is the IL with the highest solubility of CO_2 [118], it does not show an optimal behaviour as CO_2 electroreduction enhancer.

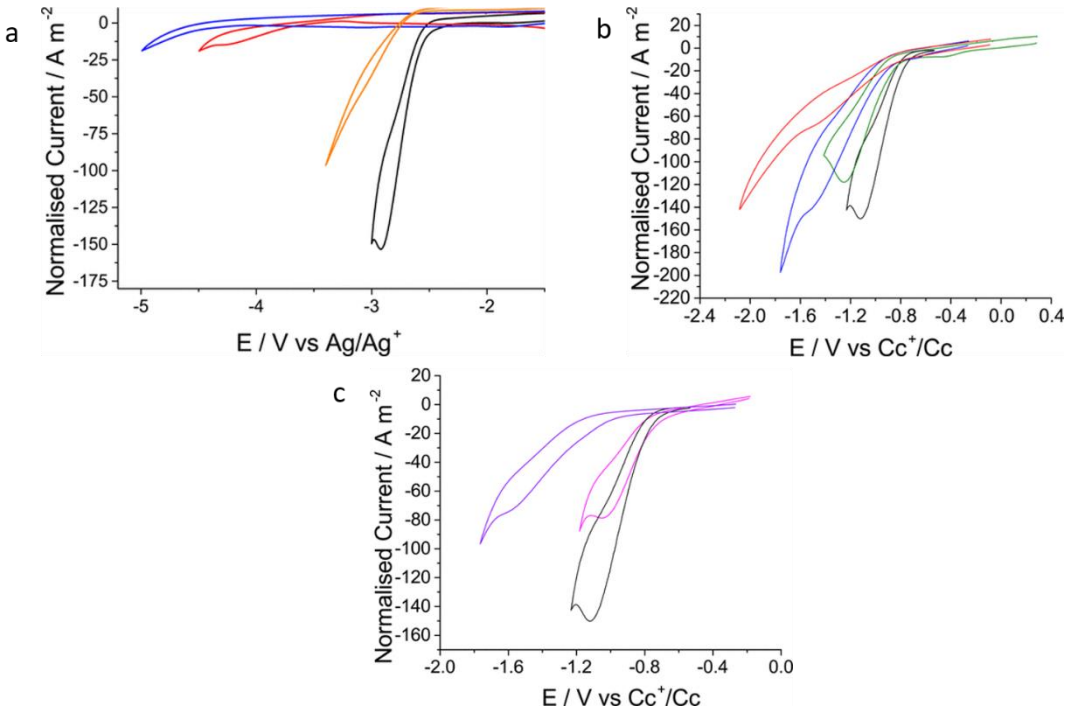

Figure 10 *a) CV of [Bmim][NTf_2] on silver (black), gold (red), platinum (orange) and glassy carbon (blue) electrodes. b) CV of CO_2 reduction on silver where ILs cation varied: black [Bmim][NTf_2], green [Bmpyrr][NTf_2], blue [Emim][NTf_2] and red [Pmim][NTf_2]. c) CV of CO_2 reduction on silver where the ILs anion varied: black [Bmim][NTf_2], pink [Bmim][BF_4], purple [Bmim][FAP]. Reprinted with permission from [115].*

The conversion efficiency of CO_2 into CO in [Bmim][BF_4] aqueous solution [119] has been investigated in some works. For instance Zhou *et al.* [120] obtained a FE for CO of 70% while, changing the anionic part to chloride, they got the best selectivity for CO with Ag electrode [104]. Also they analised the detrimental effect of the viscosity on the electrochemical selectivity for CO. The viscosity of the IL is the main limiting factor in the reagent mass transport. Increasing the percentage of water in the solution means to decrease the viscosity and increase the conductivity, but it makes the CO_2 solubility lower and favor the H_2O reduction. In Table 1 the effect of H_2O concentration on CO_2RR and HER are reported as selectivity for CO and H_2 in [Bmim][Cl] [104].

[Emim][OTf]/H_2O is a further IL previously studied for the CO_2 conversion into CO in aqueous solution giving good selectivity, despite high concentration was required [114, 121]. Welch *et al.* [110] tried to improve the mass transport in [Emim][OTf]/H_2O using elevated CO_2 pressures. Many ionic liquids have shown a decreasing in viscosity when are subjected to high pressure due to their volumetric expansion [122, 123]. In particular a positive shift in the onset potential and a large increase in the electrocatalytic current for CO_2 reduction occur when the pressure become larger.

In literature, there is not any proof-of-concept of a system performing both CO_2 capture and conversion using ILs as sorbent agent and electrolyte as well. In fact, the different studies have been performed separately on a specific ionic liquid as conversion enhancer or as sorbent agent. Since [Emim][OTf]/H_2O has been already studied for both the processes [110, 124] it could represent the right solution for a future integration between capture and electrochemical conversion in a ILs-based system. However, such perspective must take into account the absorption selectivity for CO_2 with respect to the other components of flue gas. In general, although N_2 and O_2 has weak solubility in ILs [125], it is known that SO_2 has stronger interactions with ILs than CO_2 does [126], despite the absorption of CO_2 in ILs under the exposure of SO_2 is still under investigation.

Table 1 *Influence of the water concentration in the [Bmim][Cl]/H_2O [104] solution on the CO and H_2 selectivities [120].*

H_2O concentration	CO selectivity	H_2 selectivity
20 %	>99 %	-
40 %	99 %	1 %
60 %	70 %	30 %
70 %	50 %	50 %

4. Solar-driven electrochemical CO_2 reduction

Photovoltaic-Electrochemical cells (PV-ECs) derive from the coupling between solar cell modules and electrochemical cells for the CO_2 reduction (Figure 11a). The maturity of the technologies involved [127] makes these devices suitable for scalability, stability and improved control of the efficiency of the single components. On the other hand, the main challenge regarding PV-ECs is related to the electrical operating point: in order to avoid losses and underperformances, in fact, both current and voltage must match between PV and EC modules. This matching can be achieved by engineering the single components such that the current-voltage curves cross each other at the desired operational point (Figure 11b) [128]. For instance, the I-V characteristics can be adjusted by tuning the number of solar cells for the PV module, or by changing the electrode area, catalyst material, cell volumes or electrolyte concentration in the EC module. In any case, in order to maximize the solar-to-fuel efficiency, the voltage-current point must be defined such that the PV works close to its maximum power point and the EC has its maximum selectivity for the desired products. Before reviewing the main PV-EC systems reported in the literature (section 4.3), in the following, an introduction on PV I-V characteristics and technologies will be given.

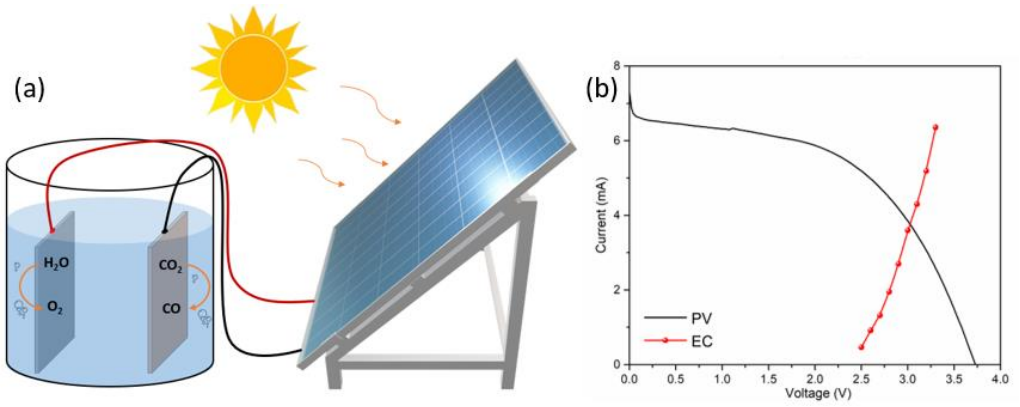

Figure 11 *(a) Schematic representation of a PV-EC device. (b) I-V characteristic of the PV module (black) and EC (red). Reprinted with permission from [128].*

4.1 Solar cell I-V characteristics

A solar cell is a diode in which the photogeneration of carriers (electron, holes) adds a "light current" component I_L (photocurrent) to the "dark current" of the diode without illumination. Therefore, under illumination, the photocurrent I_L shifts the I-V curve of the diode, such that a positive power P can be extracted.

A qualitative representation of the I-V characteristics of a solar cell is depicted in Figure 12. When evaluating the PV performance, there are some fundamental electrical parameters to consider: the open-circuit voltage V_{OC}, the short-circuit current I_{SC} and the fill factor FF. In particular, the FF defines the quality of the solar cell, by comparing the maximum power point that can be obtained (P_{MP}) with the power retrieved by the I_{SC} and V_{OC} product (P_{MAX}):

$$FF = \frac{P_{MP}}{P_{max}} = \frac{P_{MP}}{V_{OC}I_{SC}} \tag{10}$$

Lastly, the PhotoConversion Efficiency (PCE) defines the amount of electrical power generated for a given incident optical power:

$$PCE = \frac{V_{OC} I_{SC} FF}{P_{in}} \quad (11)$$

The standard test conditions for the solar cells are 1.5 AM or 1-sun illumination (i.e. incident power P_{in} of 1000 W/m^2), temperature of 25 °C and absence of wind.

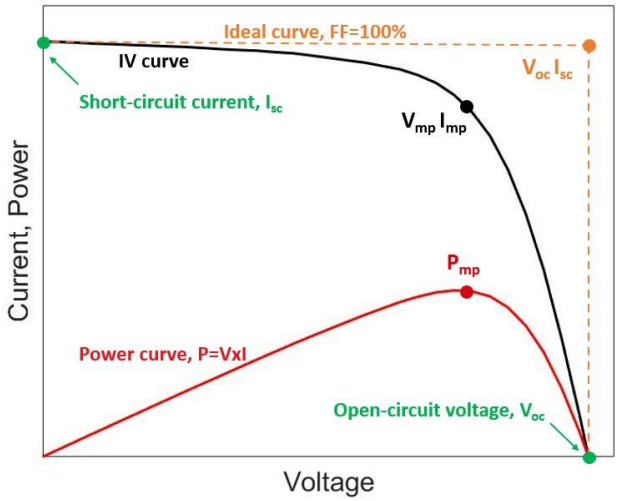

Figure 12 *Sketch of the current-voltage characteristic for a generic solar cell under illumination.*

4.2 Solar cell generations

PV is a well-established sector which takes advantage of a 50-year period of improvement and development [129]. Although different technologies are available today, it is important to carefully choose the PV component for the PV-EC system, since its output determines the solar-to-carbon conversion efficiency in the device.

The first-generation PVs are represented by wafer-based solar cells, which include single or multi-crystalline Si, characterized by high $/W cost [130], which is a crucial point considering the low-cost target for the PV-EC device.

Second generation PVs get rid of the bulk structure in favor of a thin-film technology. Typical materials used are amorphous or polycrystalline Si (a-Si, p-Si), Cadmium Telluride (CdTe), Copper Indium Gallium Diselenide (CIGS) [131] deposited on either cheap glass substrates, flexible plastic backing or transparent conductive oxides (TCOs). The thin-film solar cells are promising in terms of low-cost manufacturing in large scale production.

The third generation PVs exceed the limitations given by single-junction devices, by introducing new emerging concepts. For instance, tandem cells consist of a multijunction of individual photoactive cells stacked on top of one another, allowing a wider range of wavelengths to be absorbed. Dye sensitized solar cells (DSSCs), in contrast with the conventional cells based on semiconductive materials, are photoelectrochemical devices which separate the photogeneration of charges and the charge transport mechanisms: they gained a lot of attention thanks to their low manufacturing costs and eco-friendly materials [132-134]. Lastly, the Perovskite solar cells (PSCs) take advantage of perovskite-structured crystals as the energy-harvesting active materials. Typical materials include organic-inorganic metal halide perovskites ($CH_3NH_3PbX_3$) [135-137], where X are halogen ions like Br, Cl or I.

In PV-EC devices, the solar cell influences strongly the solar-to-carbon efficiency η_{stc}, defined as [138]:

$$\eta_{stc} = \frac{\mu_{th} \times J_{op}}{P_{in}} \times FE \quad (12)$$

where J_{op} is the operational current density and μ_{th} the thermodynamic potential (e.g. μ_{th} = 0.11 V for CO). Unless otherwise specified, all the solar-to-carbon conversions reported in this review refer to the production

of CO. The η_{stc} describes the efficiency of the PV-EC device in exploiting solar energy for the production of chemical fuels: it is therefore important to both choose the right PV technology and to retrieve the maximum efficiency possible regarding the photogeneration of carriers. As an example, in a work of Gurudayal *et al.* [139], photoelectrochemical CO_2 conversion was performed with two different PV systems, in order to address the effect of the solar cells in the final performance. In the first case (TD1), two commercial Si solar cells were exploited in series (V_{oc} of 1.1 V and I_{SC} of 61.3 mA at 1-sun illumination), while in the second configuration (TD2) two laboratory-fabricated III-V Si tandem cells were used (V_{oc} of 1.4 V and I_{SC} of 33.4 mA at 1-sun illumination): in both systems, power matching was retrieved by a maximum power point (MPP) tracker. The CO_2 reduction is performed in the EC module with IrO_2 nanotubes as anode, CuAg as cathode and a $CsHCO_3$ electrolyte of different concentrations (from 0.1 M up to 0.5 M). In the TD1 case, a η_{stc} of 3.9% was reached, while a η_{stc} of 5.6% was achieved with the TD2 configuration: the work showed clearly that the PV device plays a big role in the output of the whole PV-EC system.

4.3 Solar-driven CO production

In this section, the main works proposed in literature regarding the conversion of CO_2 in CO, by means of PV-EC systems, are reported, grouped by the electrochemical cell setup employed.

The simplest configuration is given by the single cell setup (already shown in Figure 1a). In this framework, one of the first works was performed by Schreier *et al.* [140] in 2015. In this research, they exploited a series of three perovskite solar cells (for a total V_{oc} of 3.1 V and I_{sc}=1.65 mA) as energy harvesting system, coupled with an electrochemical single cell operating at a current I_{op}≈1.65 mA. Details about the PV-EC device and the energy diagram are depicted in Figure 13. Despite the problem of crossover of dissolved products, the authors chose to implement a single cell compartment without ion-exchange membrane, to avoid overpotentials related to pH gradients at the membrane interfaces. A CO_2-saturated 0.5 M $NaHCO_3$ electrolyte is used for ion conduction, IrO_2 as anode for the OER and Au at the cathode as CO_2RR catalyst. The device reached a FE ≈ 90% and a η_{stc} > 6.5% at 2 V operating voltage for 18 hours: the experiment showed that such PV-EC systems are stable in extended operation under load, paving the way for further improvements.

Arai *et al.* [141] (2019) demonstrated a 3.4% solar-to-CO conversion by coupling six polycrystalline Si photovoltaics cells to earth-abundant catalysts for CO_2RR. A Mn-complex polymer ([Mn-MeCN], area=3.24 cm^2) on multi-wall carbon nanotubes has shown a high activity towards CO production with FE > 80%, at *ca.* 5 mA in a single cell. A triple-junction amorphous Si cell has been exploited as well and implemented in the photocathode, reporting the possibility of future monolithic artificial photosynthesis systems. In 2021, the same group [142] proposed different supports for the Mn-complex polymer previously studied [141]. In particular, by using the same set-up with poly-Si solar cells and same electrical working conditions, they showed that carbon nanohorns (CNHs) provide a better support with respect to carbon nanotubes for [Mn-MeCN]. The authors report that the CNHs enable to achieve a 3.3% η_{stc} (almost as high as the previous reported device by Arai *et al.*) with smaller electrode area (1 cm^2 against 3.14 cm^2).

Finally, for the first time in literature, Sacco *et al.* demonstrated experimentally a fully integrated PV-EC device [128]. A module of five DSSCs (V_{oc}=3.73 V, I_{sc} =7 mA) shares the Pt electrode at the cathode with the anode of the electrochemical cell, where OER occurs. The device was able to carry out an unassisted CO_2 reduction to CO, catalyzed by Cu-Sn cathode, with FE=78% and a η_{stc}=0.79%. Despite the lower performance, the device opened the possibility for stand-alone PV-EC systems completely integrated.

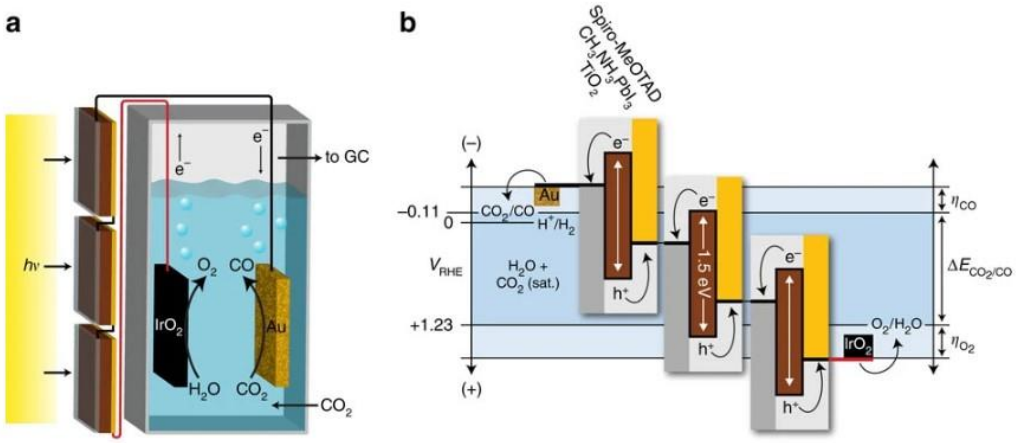

Figure 13 *(a) Graphical representation of the PV-EC device. (b) Energy diagram of the series-connected perovskite cells and the CO_2-CO conversion, with the related overpotentials (η_{O_2}, η_{CO}) and reaction free energy (ΔE). Reprinted with permissions from [140].*

For what concerns PV-EC systems with based on H-type cells (shown in Figure 1b), in a work by Schreier *et al.* [143], a triple junction GaInP/GaInAs/Ge (PCE of 28.5% at 2.24 V) solar cell is exploited as PV, while SnO_2-modified CuO nanowires are used as catalyst for both cathodic and anodic compartments. In this case, an ion exchange membrane divides the anodic and cathodic compartments, and 0.1 M $CsHCO_3$ and 0.25 M CsOH solutions were used as catholyte and anolyte, respectively. In this PV-EC device, they were able to achieve a FE ≈ 81% and η_{stc}=13.4%, doubling therefore the previous performance. In the same year, as already discussed in the previous section, Gurudayal *et al.* demonstrated the importance of the PV device in the final η_{stc} of the whole PV-EC system [139].

Chung *et al.* [144] exploited a series of three perovskite solar cells connected to Co-Pi and Au dendrites electrodes for OER and CO_2RR respectively. At a I_{op}=2.1 mA, they achieved a FE=80% and a η_{stc}>8% for CO production. Similarly, Bae *et al.* [145] chose a series of three triple-junction Si PV connected to IrO_2 and nanoporous Au catalysts for OER and CO_2RR respectively, reaching a FE=100% and η_{stc}=5.3%.

In order to lower the production costs and obtain more environmentally friendly devices exploiting earth-abundant electrocatalysts, Zhang *et al.* [146] used a custom-built large-area $[Cs_{0.05}(FA_{0.85}MA_{0.15})_{0.95}]_{Pb0.9}(I_{0.85}Br_{0.15})_3$ (CsFAMA)-based perovskite solar cell (V_{op}=4.6 V, I_{sc}=4.3 mA), single-atom Co anchored on Zr_6-cluster-porphyrin framework hollow nanocapsules (Co-SAs/Zr-CPF) as low-cost catalyst for CO_2RR and RuO_2 on carbon paper as OER catalyst. Thanks to the hollow morphology and dispersed Co single atoms of Co-SAs/Zr-CPF, the catalyst showed high activity in the CO_2-to-CO conversion, reaching a η_{stc}=12.5%.

Thanks to the employment of ion exchange membranes, and by implementing different components and stages to the PV-EC, it is also possible to exploit these devices for more complicated applications. In 2018, Wang *et al.* [147] created a redox-medium-assisted system capable of mimicking the light and dark reactions occurring in green plants. In particular, the photogenerated electrons by InGaP/GaAs/Ge PV (V_{oc}=2.54 V, I_{sc}=4.38 mA) are stored in a zinc/zincate (Zn/Zn(II)) redox pair, in which electrons can be controllably released for the spontaneous reduction of CO_2. With nano-gold and nickel-iron hydroxides as catalysts for CO_2RR and OER respectively, they managed to achieve a FE ≈ 92% and a η_{stc} =15.6% at a fixed current of 3.2 mA. A graphical representation of the system is depicted in Figure 14.

With a different approach, a PV-EC system has been designed to obtain simultaneous conversion of CO_2 and H_2S into CO and S [148]. Powered by a single three-junction Si solar cell, CO is produced through CO_2 reduction at the cathode, while a redox couple (EDTA-Fe^{2+} / EDTA-Fe^{3+}) is oxidized in the anodic compartment through electrolysis: the chemical energy stored in the solution enables the conversion of H_2S in S and protons, which flow through the bipolar membrane and close the circuit.

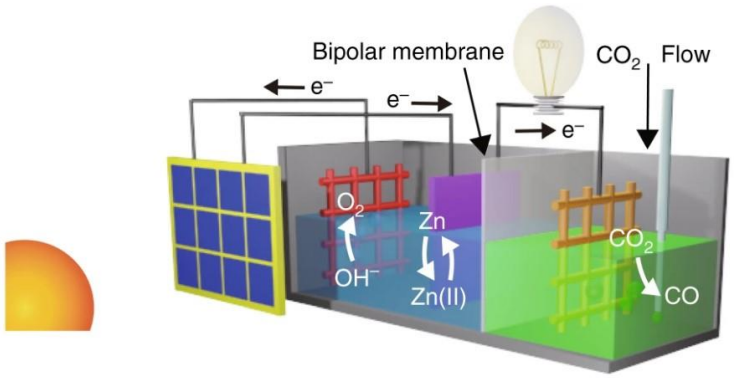

Figure 14 *Redox-medium assisted CO_2 solar-driven reduction. Reprinted with permissions from [147].*

Many efforts have been made to increase the performance and in particular the solar-to-carbon efficiencies by means of GDEs, in the flow type ECs (shown in Figure 1c). In a work of Kim *et al.* [149], Au clusters are anchored on the microporous layer of the GDE, in which gaseous CO_2 is converted in CO: a NiFe inverse opal (IO) serves as OER catalyst, in a 3 M KOH electrolyte. The device, coupled with a GaInP/GaAs solar cell, recorded high values of FE > 90% and η_{stc} =18% in a 100% CO_2 gas stream, and η_{stc} =15.9% in a stream of 10% CO_2 (typical concentration in flue gases). The authors report that, in order to exploit the higher current densities achievable by means of GDEs, it is important to use larger PV areas for high CO partial current densities (> 200 mA/cm^2).

Cheng *et al.* [150] exploited the flow cell structure as well, with GaInP/GaInAs/Ge PV (V_{oc}=2.6 V, I_{sc}=4.37 mA), Ni as anode in 1 M KOH and Ag nanoparticles on the GDE at the cathode. In order to prevent flooding, the authors chose to mount the cathode such that Ag-NP face the CO_2 gas stream in a reverse-assembled GDE. With a current density of 4.5 mA, the device managed to reach a FE=99% and a η_{stc} =19.1% using a simulated AM 1.5G sun illumination at 1 sun, and η_{stc}=18.7% under outdoor light conditions at noon.

In 2022, Wang *et al.* [151] investigated a single-atom Co-N-C catalyst for solar-driven reduction of CO_2, with CoN_4 sites supported on a carbon black (CoN_4-CB) acting as GDE for the flow cell. Coupled with a commercial a-Si PV (V_{oc}=3.51 V, I_{sc}=103 mA), and with Ni foam as catalyst for the OER compartment, the device exhibited a FE≈92.1% and a η_{stc}=4.9%, operating at a I_{op}=99.2 mA. For a better understanding of the device and all the parameters of interest, in Figure 15 the experimental set-up, I-V characteristics and efficiencies of the PV-EC system are reported.

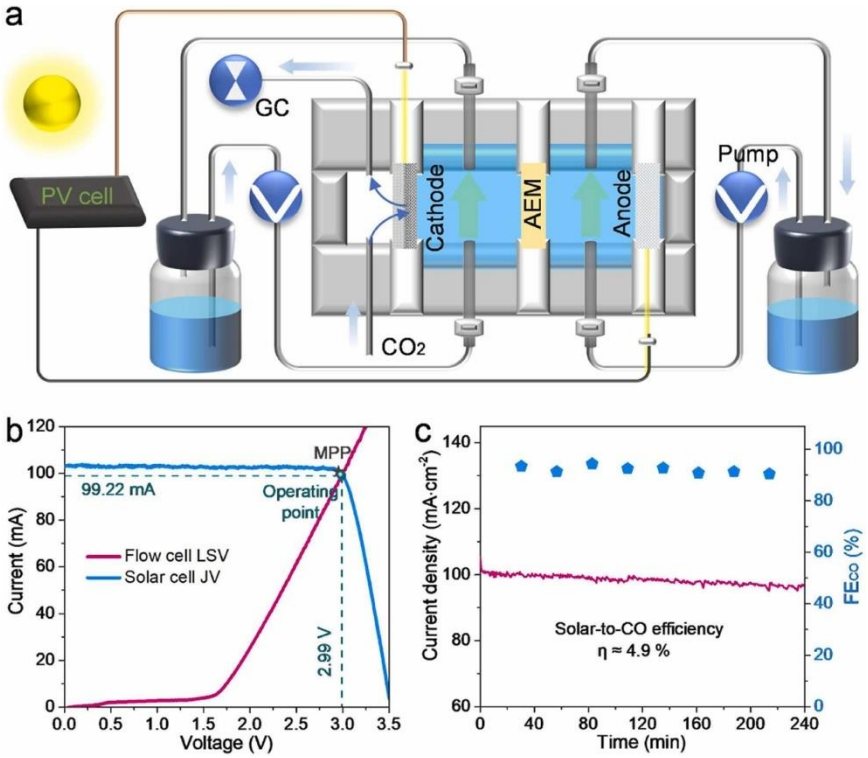

Figure 15 *(a) Set-up of the PV-EC system with flow cell. (b) I-V characteristics of the PV and EC cells at 1 sun illumination, and operating point. (c) Stability test reporting current density and FE as a function of the time of the experiment. Reprinted with permissions from [151].*

Finally, exploiting the zero-gap technology (shown in Figure 1d), Lee *et al.* [152] fabricated a large-scale PV-EC device with silicon-based solar cells with an area of 120 cm^2, obtaining a η_{stc} =12.1% and FE=99% with an outstanding current of ≈ 1 A (J_{op} ≈ 9.2 mA/cm^2 normalized on the PV illuminated surface). In this study, to match the high current retrieved by the PV, a zero-gap cell is used as CO_2 electrolyzer, with tungsten-seed-based silver dendrite (W@AgD/C) as CO_2RR catalyst, Fe-doped Co foam as OER catalyst and 1 M KOH electrolyte. The authors operated the device in real-world conditions as well, on the rooftop of a building: in these conditions, the current was found to be proportional to the solar radiation fluctuations, suggesting that the system is suitable for commercial applications. In Figure 16 it is reported the schematic representation of the PV-EC device with the zero-gap electrochemical cell.

Table 2 summarizes the main parameters of interest regarding the PV-EC devices studied in this present review, highlighting the PV technology, the electric operating point (V_{op}, I_{op}), the electrochemical cell configuration and its electrodes, the Faradaic and solar-to-CO efficiencies. It is important to emphasize that there is a lack of standardization in the specification of the current value at which the PV-EC is working: often, in literature, the current density is provided, but it is not always clear whether it refers to the PV or the EC electrodes. In this review, it has been chosen to report the values of the current intensity I_{op} and propose it as the standard value for the current specification in PV-EC devices.

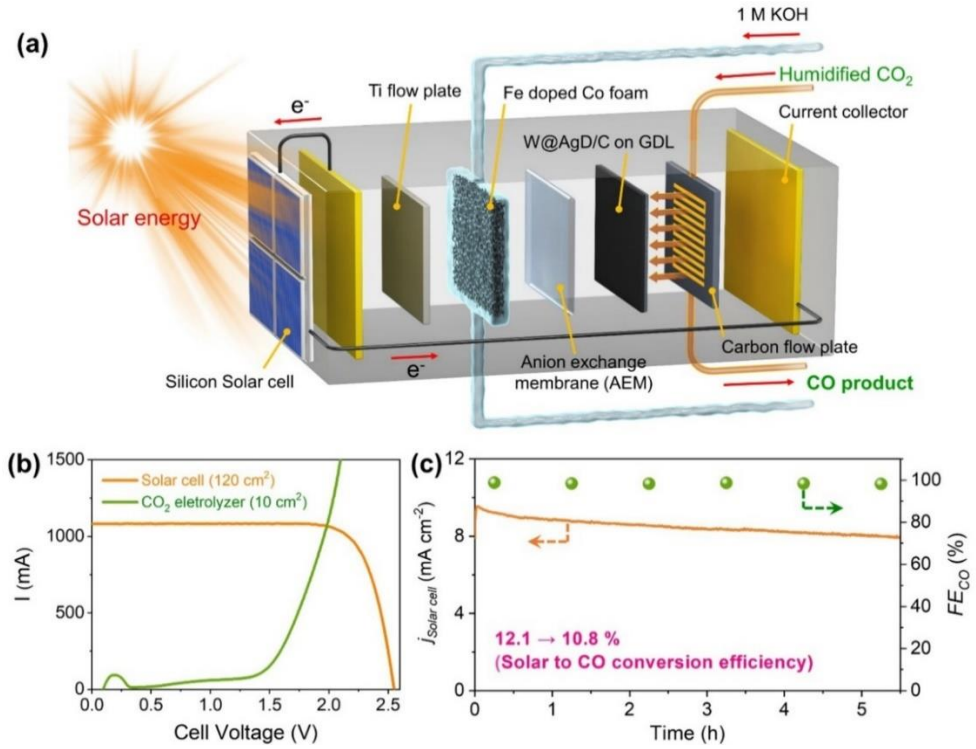

Figure 16 *(a) Graphical representation of the PV-EC device with zero-gap cell. (b) I-V characteristics of the PV and EC cells at 1 sun illumination, and operating point. (c) Stability test reporting current density and FE as a function of the time of the experiment. Reprinted with permissions from [152].*

Table 2 *Specification of the PV-EC devices, under 1 sun illumination. The "-" sign replaces data not reported in the articles.*

PV (active area)	V_{op} [V]	I_{op} [mA]	EC	OER catalyst (area)	CO_2RR catalyst (area)	FE [%]	η_{stc} [%]	Ref.
3 series-connected Perovskite (0.285 cm^2)	2.00	1.6	Single	IrO_2 (4.5 cm^2)	Au (1 cm^2)	90	>6.5	Schreier *et al.* (2015) [140]
6 series-connected poly-Si (1.6 cm^2)	2.19	5.1	Single	β-FeOOH:Ni/a-Ni(OH) (2 cm^2)	[Mn-MeCN] (3.24 cm^2)	82	3.4	Arai *et al.* (2019) [141]
Poly-Si (1.6 cm^2)	2.12	5.1	Single	Ni-doped β-FeOOH (2 cm^2)	CP/CNH/ [Mn-MeCN] (1 cm^2)	-	3.3	Nishi *et al.* (2021) [142]
DSSC module – integrated (-)	3.00	3.6	Single	Pt (-)	Cu-Sn (1 cm^2)	78	0.8	Sacco *et al.* (2020) [128]
GaInP/GaInAs/Ge (0.563 cm^2)	2.38	6.5	H-type	CuO NW (20 cm^2)	CuO NW (20 cm^2)	81	13.4	Schreier *et al.* (2017) [143]
3 series-connected Perovskite (0.282 cm^2)	2.68	2.1	H-type	Co-Pi (6.25 cm^2)	Au (0.025 cm^2)	80	>8.0	Chung *et al.* (2022) [144]
3 triple-junction Si (18 cm^2)	2.70	72.0	H-type	IrO_2 (-)	Au (1 cm^2)	100	5.3	Bae *et al.* (2022) [145]
CsFAMA-based perovskite (0.48 cm^2)	3.20	3.2	H-type	RuO_2/C (-)	Co-SAs/Zr-CPF (-)	-	12.5	Zhang *et al.* (2022) [146]
InGaP/GaAs/Ge (0.25 cm^2)	1.96	3.2	H-type	NiFe hydroxide (0.3 cm^2)	Au (0.3 cm^2)	92	15.6	Wang *et al.* (2018) [147]
Triple-junction Si (-)	-	-	H-type	Graphene (-)	Graphene-encapsulated ZnO (-)	-	7.5	Ma *et al.* (2018) [148]
GaInP/GaAs (1 cm^2)	1.63	14.1	Flow	NiFe IO (-)	Au (2 cm^2)	>90	18.0	Kim *et al.* (2020) [149]
GaInP/GaInAs/Ge (0.31 cm^2)	2.23	4.5	Flow	Ni (0.31 cm^2)	Ag (0.31 cm^2)	99	19.1	Cheng *et al.* (2020) [150]
a-Si (25 cm^2)	2.99	99.2	Flow	Ni foam (1 cm^2)	CoN_4-CB (1 cm^2)	92	4.9	Wang *et al.* (2022) [151]
Si (120 cm^2)	-	1100.0	Zero-gap	Fe-doped Co foam (10 cm^2)	W@AgD/C (10 cm^2)	99	12.1	Lee *et al.* (2021) [152]

5. Conclusion and future perspectives

In this review, we collected and analyzed the main options proposed in the literature to introduce in the market scenario a new kind of platform able to play an important role toward a closed carbon circle, valorizing CO_2 without further emissions in the atmosphere. In particular, three techniques have been introduced to integrate the carbon capture and utilization, making possible to avoid expensive processes such as compression and transportation of gaseous CO_2, necessary for instance in carbon capture and sequestration. Among these strategies, CO_2RR from (bi)carbonate solutions emerges as the most promising one. In fact, different from amine-based processes, it does not include toxic agents; moreover, it demonstrated to be able to provide good FE_{CO}. However, there is still room to work on this new solution, in terms of set-up and catalyst, to increase current and FE_{CO} and reach the performance already obtained with zero-gap electrolyzer for humidified CO_2. On the other hand, the utilization of ionic liquids has not been deeply investigated yet. Although they probably would introduce new issues related to the high viscosity and the low conductivity, a thorough investigation can be performed in order to find a suitable IL able to be employed both as capturing agent for CO_2 and as catalyst for eCO_2RR.
Regarding the solar-driven CO_2 reduction, PV-EC systems are captivating due to the conversion of CO_2 in fuels by means of renewable energy sources, in a scalable and marketable device. Here we covered the progress of this technology throughout the years, highlighting the trend of the solar-to-CO efficiencies and electrical operational points. Different EC setups have been proposed in literature (cell configuration, ORR/CO_2RR catalysts etc…), along with various PV design and generations, focusing the attention on the I-V characteristics. Current State-of-the-art η_{stc} of ≈ 19.1% has been achieved in a flow-cell configuration, while astonishing currents of ≈ 1.1A have been retrieved by exploiting a large-scale Si solar cell and newer zero-gap cell. In this framework, to reach the current-density requirements for industrialization and large-scale production, PVs should be able to match the high currents of more innovative EC setups. Moreover, energy storage systems should be taken into consideration as well, in order to guarantee continuity in the energy supply to the electrolytic cell in not optimal light conditions (e.g. clouds passing by, or at nighttime). In fact, despite one of the purposes of CO_2 valorization driven by renewable energy sources is to convert the discontinuous electrical energy into chemical energy that can be easily stored, especially when considering the hard-to-abate sectors, the solar-driven electrochemical capture and valorization represents an intriguing solution toward decarbonization. In this framework, the employment of a power management circuit could be a possible solution to couple batteries with the PV-EC device for stand-alone systems.
Finally, considering the different technologies analyzed in this review, it appears that the level of maturity achieved in each of them makes it feasible to design and implement a solar-powered electrochemical system that would enable the coupling of CO_2 capture with its valorization.

Acknowledgments

The author Matteo Agliuzza would like to thank the Italian Ministry of Education (MIUR) for the funding in the framework of the National Operational Program (PON) “Research and Innovation”.

References

[1] Houghton J. Global warming. Reports on Progress in Physics 2005;68:1343-403. 10.1088/0034-4885/68/6/r02
[2] Cook J, Nuccitelli D, Green SA, Richardson M, Winkler B, Painting R, et al. Quantifying the consensus on anthropogenic global warming in the scientific literature. Environmental Research Letters 2013;8:024024. 10.1088/1748-9326/8/2/024024
[3] IPCC. Fifth Assessment Report. 2014. https://www.ipcc.ch/assessment-report/ar5/

[4] EuropeanCommission. Paris Agreement. 2015. https://ec.europa.eu/clima/eu-action/international-action-climate-change/climate-negotiations/paris-agreement_it
[5] EuropeanCommission. 2030 climate & energy framework. 2020. https://ec.europa.eu/clima/eu-action/climate-strategies-targets/2030-climate-energy-framework_en
[6] EuropeanCommission. COP26 conclusion. 2021. https://ec.europa.eu/commission/presscorner/api/files/document/print/en/ip_21_6021/IP_21_6021_EN.pdf
[7] Osman AI, Hefny M, Abdel Maksoud MIA, Elgarahy AM, Rooney DW. Recent advances in carbon capture storage and utilisation technologies: a review. Environmental Chemistry Letters 2021;19:797-849. 10.1007/s10311-020-01133-3
[8] Al-Mamoori A, Krishnamurthy A, Rownaghi AA, Rezaei F. Carbon Capture and Utilization Update. Energy Technology 2017;5:834-49. https://doi.org/10.1002/ente.201600747
[9] Baena-Moreno FM, Rodríguez-Galán M, Vega F, Alonso-Fariñas B, Vilches Arenas LF, Navarrete B. Carbon capture and utilization technologies: a literature review and recent advances. Energy Sources, Part A: Recovery, Utilization, and Environmental Effects 2019;41:1403-33. 10.1080/15567036.2018.1548518
[10] Ghiat I, Al-Ansari T. A review of carbon capture and utilisation as a CO2 abatement opportunity within the EWF nexus. Journal of CO2 Utilization 2021;45:101432. https://doi.org/10.1016/j.jcou.2020.101432
[11] GlobalCCSInstitute. World's largest capture pilot plant for cement commissioned in China. 2018. https://www.globalccsinstitute.com/news-media/insights/worlds-largest-capture-pilot-plant-for-cement-commissioned-in-china/
[12] LafargeHolcim. LafargeHolcim launches carbon capture project in Canada. 2019. https://www.lafargeholcim.com/lafargeholcim-launch-carbon-capture-project-canada
[13] EuropeanCommission. Successful demonstration of CO2 separation at Project LEILAC in Belgium. 2019. https://www.project-leilac.eu/successful-co2-separation
[14] Norcem. CCS at Norcem Brevik: Background. 2021. https://www.norcem.no/en/CCS%20at%20Brevik
[15] Lehigh. LEHIGH CEMENT AND THE INTERNATIONAL KNOWLEDGE CENTRE PIONEERING A FEASIBILITY STUDY OF FULL-SCALE CARBON CAPTURE STORAGE (CCS) ON CEMENT. 2019. https://www.lehighhanson.com/resources/news/news/2019/11/28/lehigh-cement-and-the-international-knowledge-centre-pioneering-a-feasibility-study-of-full-scale-carbon-capture-storage-(ccs)-on-cement
[16] EuropeanCommission. Recycling carbon dioxide in the cement industry to produce added-value additives: a step towards a CO2 circular economy. 2017. https://cordis.europa.eu/project/id/768583
[17] Sreenivasulu B, Gayatri DV, Sreedhar I, Raghavan KV. A journey into the process and engineering aspects of carbon capture technologies. Renewable and Sustainable Energy Reviews 2015;41:1324-50. https://doi.org/10.1016/j.rser.2014.09.029
[18] Ben-Mansour R, Habib MA, Bamidele OE, Basha M, Qasem NAA, Peedikakkal A, et al. Carbon capture by physical adsorption: Materials, experimental investigations and numerical modeling and simulations – A review. Applied Energy 2016;161:225-55. https://doi.org/10.1016/j.apenergy.2015.10.011
[19] Khalilpour R, Mumford K, Zhai H, Abbas A, Stevens G, Rubin ES. Membrane-based carbon capture from flue gas: a review. Journal of Cleaner Production 2015;103:286-300. https://doi.org/10.1016/j.jclepro.2014.10.050
[20] Wilberforce T, Olabi AG, Sayed ET, Elsaid K, Abdelkareem MA. Progress in carbon capture technologies. Science of The Total Environment 2021;761:143203. https://doi.org/10.1016/j.scitotenv.2020.143203
[21] Gentry PR, House-Knight T, Harris A, Greene T, Campleman S. Potential occupational risk of amines in carbon capture for power generation. International Archives of Occupational and Environmental Health 2014;87:591-606. 10.1007/s00420-013-0900-y
[22] Latini G, Signorile M, Rosso F, Fin A, d'Amora M, Giordani S, et al. Efficient and reversible CO2 capture in bio-based ionic liquids solutions. Journal of CO2 Utilization 2022;55:101815. https://doi.org/10.1016/j.jcou.2021.101815

[23] Xing Y, Ma Z, Su W, Wang Q, Wang X, Zhang H. Analysis of Research Status of CO2 Conversion Technology Based on Bibliometrics. Catalysts 2020;10:370.
[24] Sacco A. Electrochemical impedance spectroscopy as a tool to investigate the electroreduction of carbon dioxide: A short review. Journal of CO2 Utilization 2018;27:22-31. https://doi.org/10.1016/j.jcou.2018.06.020
[25] Xu L, Xiu Y, Liu F, Liang Y, Wang S. Research Progress in Conversion of CO2 to Valuable Fuels. Molecules 2020;25:3653.
[26] Artz J, Müller TE, Thenert K, Kleinekorte J, Meys R, Sternberg A, et al. Sustainable Conversion of Carbon Dioxide: An Integrated Review of Catalysis and Life Cycle Assessment. Chemical Reviews 2018;118:434-504. 10.1021/acs.chemrev.7b00435
[27] Samanta S, Srivastava R. Catalytic conversion of CO2 to chemicals and fuels: the collective thermocatalytic/photocatalytic/electrocatalytic approach with graphitic carbon nitride. Materials Advances 2020;1:1506-45. 10.1039/D0MA00293C
[28] Li W, Wang H, Jiang X, Zhu J, Liu Z, Guo X, et al. A short review of recent advances in CO2 hydrogenation to hydrocarbons over heterogeneous catalysts. RSC Advances 2018;8:7651-69. 10.1039/C7RA13546G
[29] Nagasawa H, Yamasaki A, Iizuka A, Kumagai K, Yanagisawa Y. A new recovery process of carbon dioxide from alkaline carbonate solution via electrodialysis. AIChE Journal 2009;55:3286-93. https://doi.org/10.1002/aic.11907
[30] Renfrew SE, Starr DE, Strasser P. Electrochemical Approaches toward CO2 Capture and Concentration. ACS Catalysis 2020;10:13058-74. 10.1021/acscatal.0c03639
[31] Xie H, Wu Y, Liu T, Wang F, Chen B, Liang B. Low-energy-consumption electrochemical CO2 capture driven by biomimetic phenazine derivatives redox medium. Applied Energy 2020;259:114119. https://doi.org/10.1016/j.apenergy.2019.114119
[32] Lu Q, Jiao F. Electrochemical CO2 reduction: Electrocatalyst, reaction mechanism, and process engineering. Nano Energy 2016;29:439-56. https://doi.org/10.1016/j.nanoen.2016.04.009
[33] Chen C, Khosrowabadi Kotyk JF, Sheehan SW. Progress toward Commercial Application of Electrochemical Carbon Dioxide Reduction. Chem 2018;4:2571-86. 10.1016/j.chempr.2018.08.019
[34] Bejtka K, Zeng J, Sacco A, Castellino M, Hernández S, Farkhondehfal MA, et al. Chainlike Mesoporous SnO2 as a Well-Performing Catalyst for Electrochemical CO2 Reduction. ACS Applied Energy Materials 2019;2:3081-91. 10.1021/acsaem.8b02048
[35] Qiao J, Liu Y, Hong F, Zhang J. A review of catalysts for the electroreduction of carbon dioxide to produce low-carbon fuels. Chemical Society Reviews 2014;43:631-75. 10.1039/C3CS60323G
[36] Mezza A, Pettigiani A, Monti NBD, Bocchini S, Farkhondehfal MA, Zeng J, et al. An Electrochemical Platform for the Carbon Dioxide Capture and Conversion to Syngas. Energies 2021;14:7869.
[37] Welch AJ, Dunn E, DuChene JS, Atwater HA. Bicarbonate or Carbonate Processes for Coupling Carbon Dioxide Capture and Electrochemical Conversion. ACS Energy Letters 2020;5:940-5. 10.1021/acsenergylett.0c00234
[38] Savino U, Sacco A. Tandem devices for simultaneous CO2 reduction at the cathode and added-value products formation at the anode. Journal of CO2 Utilization 2021;52:101697. https://doi.org/10.1016/j.jcou.2021.101697
[39] Bushuyev OS, De Luna P, Dinh CT, Tao L, Saur G, van de Lagemaat J, et al. What Should We Make with CO2 and How Can We Make It? Joule 2018;2:825-32. https://doi.org/10.1016/j.joule.2017.09.003
[40] Zeng J, Castellino M, Bejtka K, Sacco A, Di Martino G, Farkhondehfal MA, et al. Facile synthesis of cubic cuprous oxide for electrochemical reduction of carbon dioxide. Journal of Materials Science 2021;56:1255-71. 10.1007/s10853-020-05278-y
[41] Lettieri S, Zeng J, Farkhondehfal MA, Savino U, Fontana M, Pirri CF, et al. Correlation between impedance spectroscopy and bubble-induced mass transport in the electrochemical reduction of carbon dioxide. Journal of Energy Chemistry 2022;67:500-7. https://doi.org/10.1016/j.jechem.2021.10.023
[42] Jouny M, Luc W, Jiao F. General Techno-Economic Analysis of CO2 Electrolysis Systems. Industrial & Engineering Chemistry Research 2018;57:2165-77. 10.1021/acs.iecr.7b03514

[43] Kibria MG, Edwards JP, Gabardo CM, Dinh C-T, Seifitokaldani A, Sinton D, et al. Electrochemical CO2 Reduction into Chemical Feedstocks: From Mechanistic Electrocatalysis Models to System Design. Advanced Materials 2019;31:1807166. https://doi.org/10.1002/adma.201807166
[44] Lourenço MAO, Zeng J, Jagdale P, Castellino M, Sacco A, Farkhondehfal MA, et al. Biochar/Zinc Oxide Composites as Effective Catalysts for Electrochemical CO2 Reduction. ACS Sustainable Chemistry & Engineering 2021;9:5445-53. 10.1021/acssuschemeng.1c00837
[45] Nielsen DU, Hu X-M, Daasbjerg K, Skrydstrup T. Chemically and electrochemically catalysed conversion of CO2 to CO with follow-up utilization to value-added chemicals. Nature Catalysis 2018;1:244-54. 10.1038/s41929-018-0051-3
[46] Zeng J, Fontana M, Castellino M, Sacco A, Farkhondehfal MA, Drago F, et al. Efficient CO2 Electroreduction on Tin Modified Cuprous Oxide Synthesized via a One-Pot Microwave-Assisted Route. Catalysts 2021;11:907.
[47] Farkhondehfal MA, Hernández S, Rattalino M, Makkee M, Lamberti A, Chiodoni A, et al. Syngas production by electrocatalytic reduction of CO2 using Ag-decorated TiO2 nanotubes. International Journal of Hydrogen Energy 2020;45:26458-71. https://doi.org/10.1016/j.ijhydene.2019.04.180
[48] Zeng J, Rino T, Bejtka K, Castellino M, Sacco A, Farkhondehfal MA, et al. Coupled Copper–Zinc Catalysts for Electrochemical Reduction of Carbon Dioxide. ChemSusChem 2020;13:4128-39. https://doi.org/10.1002/cssc.202000971
[49] Hagos FY, Aziz ARA, Sulaiman SA. Trends of Syngas as a Fuel in Internal Combustion Engines. Advances in Mechanical Engineering 2014;6:401587. 10.1155/2014/401587
[50] Zeng J, Bejtka K, Di Martino G, Sacco A, Castellino M, Re Fiorentin M, et al. Microwave-Assisted Synthesis of Copper-Based Electrocatalysts for Converting Carbon Dioxide to Tunable Syngas. ChemElectroChem 2020;7:229-38. 10.1002/celc.201901730
[51] Schneider J, Jia H, Muckerman JT, Fujita E. Thermodynamics and kinetics of CO2, CO, and H+ binding to the metal centre of CO2reductioncatalysts. Chemical Society Reviews 2012;41:2036-51. 10.1039/C1CS15278E
[52] Feaster JT, Shi C, Cave ER, Hatsukade T, Abram DN, Kuhl KP, et al. Understanding Selectivity for the Electrochemical Reduction of Carbon Dioxide to Formic Acid and Carbon Monoxide on Metal Electrodes. ACS Catalysis 2017;7:4822-7. 10.1021/acscatal.7b00687
[53] Li X, Wang S, Li L, Sun Y, Xie Y. Progress and Perspective for In Situ Studies of CO2 Reduction. Journal of the American Chemical Society 2020;142:9567-81. 10.1021/jacs.0c02973
[54] Ahangari HT, Portail T, Marshall AT. Comparing the electrocatalytic reduction of CO2 to CO on gold cathodes in batch and continuous flow electrochemical cells. Electrochemistry Communications 2019;101:78-81. https://doi.org/10.1016/j.elecom.2019.03.005
[55] Raciti D, Mao M, Park JH, Wang C. Local pH Effect in the CO₂Reduction Reaction on High-Surface-Area Copper Electrocatalysts. Journal of The Electrochemical Society 2018;165:F799-F804. 10.1149/2.0521810jes
[56] Varela AS. The importance of pH in controlling the selectivity of the electrochemical CO2 reduction. Current Opinion in Green and Sustainable Chemistry 2020;26:100371. https://doi.org/10.1016/j.cogsc.2020.100371
[57] Gao D, Wang J, Wu H, Jiang X, Miao S, Wang G, et al. pH effect on electrocatalytic reduction of CO2 over Pd and Pt nanoparticles. Electrochemistry Communications 2015;55:1-5. https://doi.org/10.1016/j.elecom.2015.03.008
[58] Mizuno T, Adachi K, Ohta K, Saji A. Effect of CO2 pressure on photocatalytic reduction of CO2 using TiO2 in aqueous solutions. Journal of Photochemistry and Photobiology A: Chemistry 1996;98:87-90. https://doi.org/10.1016/1010-6030(96)04334-1
[59] Löwe A, Rieg C, Hierlemann T, Salas N, Kopljar D, Wagner N, et al. Influence of Temperature on the Performance of Gas Diffusion Electrodes in the CO2 Reduction Reaction. ChemElectroChem 2019;6:4497-506. https://doi.org/10.1002/celc.201900872
[60] Jianping Q, Juntao T, Jie S, Cuiwei W, Mengqian Q, Zhiqiao H, et al. Preparation of a silver electrode with a three-dimensional surface and its performance in the electrochemical reduction of carbon dioxide. Electrochimica Acta 2016;203:99-108. https://doi.org/10.1016/j.electacta.2016.03.182
[61] Kostecki R, Augustynski J. Electrochemical reduction of CO2 at an activated silver electrode. Berichte der Bunsengesellschaft für physikalische Chemie 1994;98:1510-5. https://doi.org/10.1002/bbpc.19940981203

[62] Hori Y, Konishi H, Futamura T, Murata A, Koga O, Sakurai H, et al. “Deactivation of copper electrode” in electrochemical reduction of CO2. Electrochimica Acta 2005;50:5354-69. https://doi.org/10.1016/j.electacta.2005.03.015
[63] Fan L, Xia C, Yang F, Wang J, Wang H, Lu Y. Strategies in catalysts and electrolyzer design for electrochemical CO2 reduction toward C2+ products. Science Advances 2020;6:eaay3111. 10.1126/sciadv.aay3111
[64] Tufa RA, Chanda D, Ma M, Aili D, Demissie TB, Vaes J, et al. Towards highly efficient electrochemical CO2 reduction: Cell designs, membranes and electrocatalysts. Applied Energy 2020;277:115557. https://doi.org/10.1016/j.apenergy.2020.115557
[65] Lin R, Guo J, Li X, Patel P, Seifitokaldani A. Electrochemical Reactors for CO2 Conversion. Catalysts 2020;10:473.
[66] Sharifian R, Wagterveld RM, Digdaya IA, Xiang C, Vermaas DA. Electrochemical carbon dioxide capture to close the carbon cycle. Energy & Environmental Science 2021;14:781-814. 10.1039/D0EE03382K
[67] Gurkan B, Su X, Klemm A, Kim Y, Mallikarjun Sharada S, Rodriguez-Katakura A, et al. Perspective and challenges in electrochemical approaches for reactive CO2 separations. iScience 2021;24:103422. https://doi.org/10.1016/j.isci.2021.103422
[68] Weekes DM, Salvatore DA, Reyes A, Huang A, Berlinguette CP. Electrolytic CO2 Reduction in a Flow Cell. Accounts of Chemical Research 2018;51:910-8. 10.1021/acs.accounts.8b00010
[69] Dutcher B, Fan M, Russell AG. Amine-Based CO2 Capture Technology Development from the Beginning of 2013—A Review. ACS Applied Materials & Interfaces 2015;7:2137-48. 10.1021/am507465f
[70] Iizuka A, Hashimoto K, Nagasawa H, Kumagai K, Yanagisawa Y, Yamasaki A. Carbon dioxide recovery from carbonate solutions using bipolar membrane electrodialysis. Separation and Purification Technology 2012;101:49-59. https://doi.org/10.1016/j.seppur.2012.09.016
[71] Digdaya IA, Sullivan I, Lin M, Han L, Cheng W-H, Atwater HA, et al. A direct coupled electrochemical system for capture and conversion of CO2 from oceanwater. Nature Communications 2020;11:4412. 10.1038/s41467-020-18232-y
[72] Muroyama AP, Pătru A, Gubler L. Review—CO2 Separation and Transport via Electrochemical Methods. Journal of The Electrochemical Society 2020;167:133504. 10.1149/1945-7111/abbbb9
[73] Xie H, Jiang W, Liu T, Wu Y, Wang Y, Chen B, et al. Low-Energy Electrochemical Carbon Dioxide Capture Based on a Biological Redox Proton Carrier. Cell Reports Physical Science 2020;1:100046. https://doi.org/10.1016/j.xcrp.2020.100046
[74] Jin S, Wu M, Gordon RG, Aziz MJ, Kwabi DG. pH swing cycle for CO2 capture electrochemically driven through proton-coupled electron transfer. Energy & Environmental Science 2020;13:3706-22. 10.1039/D0EE01834A
[75] Zhou Q, Zhang W, Qiu M, Yu Y. Role of oxygen in copper-based catalysts for carbon dioxide electrochemical reduction. Materials Today Physics 2021;20:100443. https://doi.org/10.1016/j.mtphys.2021.100443
[76] Qiu Y-L, Zhong H-X, Zhang T-T, Xu W-B, Su P-P, Li X-F, et al. Selective Electrochemical Reduction of Carbon Dioxide Using Cu Based Metal Organic Framework for CO2 Capture. ACS Applied Materials & Interfaces 2018;10:2480-9. 10.1021/acsami.7b15255
[77] Jens CM, Müller L, Leonhard K, Bardow A. To Integrate or Not to Integrate—Techno-Economic and Life Cycle Assessment of CO2 Capture and Conversion to Methyl Formate Using Methanol. ACS Sustainable Chemistry & Engineering 2019;7:12270-80. 10.1021/acssuschemeng.9b01603
[78] Mohsin I, Al-Attas TA, Sumon KZ, Bergerson J, McCoy S, Kibria MG. Economic and Environmental Assessment of Integrated Carbon Capture and Utilization. Cell Reports Physical Science 2020;1:100104. https://doi.org/10.1016/j.xcrp.2020.100104
[79] Li MI, E.; Montfort, H. P. I. van; Burdyny, T. . Sequential vs Integrated CO2 Capture and Electrochemical Conversion: An Energy Comparison. ChemRxiv 2021. 10.26434/chemrxiv-2021-33k4d
[80] Zouaoui N, Ossonon BD, Fan M, Mayilukila D, Garbarino S, de Silveira G, et al. Electroreduction of CO2 to formate on amine modified Pb electrodes. Journal of Materials Chemistry A 2019;7:11272-81. 10.1039/C8TA09637F

[81] Margarit CG, Asimow NG, Costentin C, Nocera DG. Tertiary Amine-Assisted Electroreduction of Carbon Dioxide to Formate Catalyzed by Iron Tetraphenylporphyrin. ACS Energy Letters 2020;5:72-8. 10.1021/acsenergylett.9b02093
[82] Pérez-Gallent E, Vankani C, Sánchez-Martínez C, Anastasopol A, Goetheer E. Integrating CO2 Capture with Electrochemical Conversion Using Amine-Based Capture Solvents as Electrolytes. Industrial & Engineering Chemistry Research 2021;60:4269-78. 10.1021/acs.iecr.0c05848
[83] Sharma SD, Azzi M. A critical review of existing strategies for emission control in the monoethanolamine-based carbon capture process and some recommendations for improved strategies. Fuel 2014;121:178-88. https://doi.org/10.1016/j.fuel.2013.12.023
[84] Krótki A, Więcław-Solny L, Tatarczuk A, Stec M, Wilk A, Śpiewak D, et al. Laboratory Studies of Post-combustion CO2 Capture by Absorption with MEA and AMP Solvents. Arabian Journal for Science and Engineering 2016;41:371-9. 10.1007/s13369-015-2008-z
[85] Bernhardsen IM, Knuutila HK. A review of potential amine solvents for CO2 absorption process: Absorption capacity, cyclic capacity and pKa. International Journal of Greenhouse Gas Control 2017;61:27-48. https://doi.org/10.1016/j.ijggc.2017.03.021
[86] Ruuskanen V, Koponen J, Huoman K, Kosonen A, Niemelä M, Ahola J. PEM water electrolyzer model for a power-hardware-in-loop simulator. International Journal of Hydrogen Energy 2017;42:10775-84. https://doi.org/10.1016/j.ijhydene.2017.03.046
[87] Camper D, Bara JE, Gin DL, Noble RD. Room-Temperature Ionic Liquid−Amine Solutions: Tunable Solvents for Efficient and Reversible Capture of CO2. Industrial & Engineering Chemistry Research 2008;47:8496-8. 10.1021/ie801002m
[88] Chen L, Li F, Zhang Y, Bentley CL, Horne M, Bond AM, et al. Electrochemical Reduction of Carbon Dioxide in a Monoethanolamine Capture Medium. ChemSusChem 2017;10:4109-18. https://doi.org/10.1002/cssc.201701075
[89] Filotás D, Nagy T, Nagy L, Mizsey P, Nagy G. Extended Investigation of Electrochemical CO2 Reduction in Ethanolamine Solutions by SECM. Electroanalysis 2018;30:690-7. https://doi.org/10.1002/elan.201700693
[90] Bhattacharya M, Sebghati S, Vercella YM, Saouma CT. Electrochemical Reduction of Carbamates and Carbamic Acids: Implications for Combined Carbon Capture and Electrochemical CO₂ Recycling. Journal of The Electrochemical Society 2020;167:086507. 10.1149/1945-7111/ab8ed0
[91] Abdinejad M, Mirza Z, Zhang X-a, Kraatz H-B. Enhanced Electrocatalytic Activity of Primary Amines for CO2 Reduction Using Copper Electrodes in Aqueous Solution. ACS Sustainable Chemistry & Engineering 2020;8:1715-20. 10.1021/acssuschemeng.9b06837
[92] Zhou S, Chen X, Nguyen T, Voice AK, Rochelle GT. Aqueous Ethylenediamine for CO2 Capture. ChemSusChem 2010;3:913-8. https://doi.org/10.1002/cssc.200900293
[93] Sahu C, Sircar A, Sangwai JS, Kumar R. Effect of Methylamine, Amylamine, and Decylamine on the Formation and Dissociation Kinetics of CO2 Hydrate Relevant for Carbon Dioxide Sequestration. Industrial & Engineering Chemistry Research 2022;61:2672-84. 10.1021/acs.iecr.1c04074
[94] Lee G, Li YC, Kim J-Y, Peng T, Nam D-H, Sedighian Rasouli A, et al. Electrochemical upgrade of CO2 from amine capture solution. Nature Energy 2021;6:46-53. 10.1038/s41560-020-00735-z
[95] Khurram A, Yan L, Yin Y, Zhao L, Gallant BM. Promoting Amine-Activated Electrochemical CO2 Conversion with Alkali Salts. The Journal of Physical Chemistry C 2019;123:18222-31. 10.1021/acs.jpcc.9b04258
[96] Ma M, Clark EL, Therkildsen KT, Dalsgaard S, Chorkendorff I, Seger B. Insights into the carbon balance for CO2 electroreduction on Cu using gas diffusion electrode reactor designs. Energy & Environmental Science 2020;13:977-85. 10.1039/D0EE00047G
[97] Watkins JD, Siefert NS, Zhou X, Myers CR, Kitchin JR, Hopkinson DP, et al. Redox-Mediated Separation of Carbon Dioxide from Flue Gas. Energy & Fuels 2015;29:7508-15. 10.1021/acs.energyfuels.5b01807
[98] Li T, Lees EW, Goldman M, Salvatore DA, Weekes DM, Berlinguette CP. Electrolytic Conversion of Bicarbonate into CO in a Flow Cell. Joule 2019;3:1487-97. https://doi.org/10.1016/j.joule.2019.05.021
[99] Li YC, Lee G, Yuan T, Wang Y, Nam D-H, Wang Z, et al. CO2 Electroreduction from Carbonate Electrolyte. ACS Energy Letters 2019;4:1427-31. 10.1021/acsenergylett.9b00975

[100] Keith DW, Holmes G, St. Angelo D, Heidel K. A Process for Capturing CO2 from the Atmosphere. Joule 2018;2:1573-94. https://doi.org/10.1016/j.joule.2018.05.006
[101] Salvatore DA, Weekes DM, He J, Dettelbach KE, Li YC, Mallouk TE, et al. Electrolysis of Gaseous CO2 to CO in a Flow Cell with a Bipolar Membrane. ACS Energy Letters 2018;3:149-54. 10.1021/acsenergylett.7b01017
[102] Li YC, Zhou D, Yan Z, Gonçalves RH, Salvatore DA, Berlinguette CP, et al. Electrolysis of CO2 to Syngas in Bipolar Membrane-Based Electrochemical Cells. ACS Energy Letters 2016;1:1149-53. 10.1021/acsenergylett.6b00475
[103] Fink AG, Lees EW, Zhang Z, Ren S, Delima RS, Berlinguette CP. Impact of Alkali Cation Identity on the Conversion of HCO3− to CO in Bicarbonate Electrolyzers. ChemElectroChem 2021;8:2094-100. https://doi.org/10.1002/celc.202100408
[104] Resasco J, Chen LD, Clark E, Tsai C, Hahn C, Jaramillo TF, et al. Promoter Effects of Alkali Metal Cations on the Electrochemical Reduction of Carbon Dioxide. Journal of the American Chemical Society 2017;139:11277-87. 10.1021/jacs.7b06765
[105] Zhang Z, Lees EW, Ren S, Mowbray BAW, Huang A, Berlinguette CP. Conversion of Reactive Carbon Solutions into CO at Low Voltage and High Carbon Efficiency. ACS Central Science 2022;8:749-55. 10.1021/acscentsci.2c00329
[106] Aghaie M, Rezaei N, Zendehboudi S. A systematic review on CO2 capture with ionic liquids: Current status and future prospects. Renewable and Sustainable Energy Reviews 2018;96:502-25. https://doi.org/10.1016/j.rser.2018.07.004
[107] Lian S, Song C, Liu Q, Duan E, Ren H, Kitamura Y. Recent advances in ionic liquids-based hybrid processes for CO2 capture and utilization. Journal of Environmental Sciences 2021;99:281-95. https://doi.org/10.1016/j.jes.2020.06.034
[108] Hallett JP, Welton T. Room-Temperature Ionic Liquids: Solvents for Synthesis and Catalysis. 2. Chemical Reviews 2011;111:3508-76. 10.1021/cr1003248
[109] Qu Y, Zhao Y, Li D, Sun J. Task-specific ionic liquids for carbon dioxide absorption and conversion into value-added products. Current Opinion in Green and Sustainable Chemistry 2022;34:100599. https://doi.org/10.1016/j.cogsc.2022.100599
[110] Welch LM, Vijayaraghavan M, Greenwell F, Satherley J, Cowan AJ. Electrochemical carbon dioxide reduction in ionic liquids at high pressure. Faraday Discussions 2021;230:331-43. 10.1039/D0FD00140F
[111] Lu W, Jia B, Cui B, Zhang Y, Yao K, Zhao Y, et al. Efficient Photoelectrochemical Reduction of Carbon Dioxide to Formic Acid: A Functionalized Ionic Liquid as an Absorbent and Electrolyte. Angewandte Chemie International Edition 2017;56:11851-4. https://doi.org/10.1002/anie.201703977
[112] Rosen Brian A, Salehi-Khojin A, Thorson Michael R, Zhu W, Whipple Devin T, Kenis Paul JA, et al. Ionic Liquid–Mediated Selective Conversion of CO2 to CO at Low Overpotentials. Science 2011;334:643-4. 10.1126/science.1209786
[113] Faggion D, Gonçalves WDG, Dupont J. CO2 Electroreduction in Ionic Liquids. Frontiers in Chemistry 2019;7. 10.3389/fchem.2019.00102
[114] Neubauer SS, Krause RK, Schmid B, Guldi DM, Schmid G. Overpotentials and Faraday Efficiencies in CO2 Electrocatalysis–the Impact of 1-Ethyl-3-Methylimidazolium Trifluoromethanesulfonate. Advanced Energy Materials 2016;6:1502231. https://doi.org/10.1002/aenm.201502231
[115] Tanner EEL, Batchelor-McAuley C, Compton RG. Carbon Dioxide Reduction in Room-Temperature Ionic Liquids: The Effect of the Choice of Electrode Material, Cation, and Anion. The Journal of Physical Chemistry C 2016;120:26442-7. 10.1021/acs.jpcc.6b10564
[116] Gomes de Azevedo R, Esperança JMSS, Szydlowski J, Visak ZP, Pires PF, Guedes HJR, et al. Thermophysical and thermodynamic properties of ionic liquids over an extended pressure range: [bmim][NTf2] and [hmim][NTf2]. The Journal of Chemical Thermodynamics 2005;37:888-99. https://doi.org/10.1016/j.jct.2005.04.018
[117] Gonzalez-Miquel M, Bedia J, Abrusci C, Palomar J, Rodriguez F. Anion Effects on Kinetics and Thermodynamics of CO2 Absorption in Ionic Liquids. The Journal of Physical Chemistry B 2013;117:3398-406. 10.1021/jp4007679
[118] Muldoon MJ, Aki SNVK, Anderson JL, Dixon JK, Brennecke JF. Improving Carbon Dioxide Solubility in Ionic Liquids. The Journal of Physical Chemistry B 2007;111:9001-9. 10.1021/jp071897q

[119] Liu W, Zhao T, Zhang Y, Wang H, Yu M. The Physical Properties of Aqueous Solutions of the Ionic Liquid [BMIM][BF4]. Journal of Solution Chemistry 2006;35:1337-46. 10.1007/s10953-006-9064-7
[120] Zhou F, Liu S, Yang B, Wang P, Alshammari AS, Deng Y. Highly selective electrocatalytic reduction of carbon dioxide to carbon monoxide on silver electrode with aqueous ionic liquids. Electrochemistry Communications 2014;46:103-6. https://doi.org/10.1016/j.elecom.2014.06.023
[121] Hailu A, Shaw SK. Efficient Electrocatalytic Reduction of Carbon Dioxide in 1-Ethyl-3-methylimidazolium Trifluoromethanesulfonate and Water Mixtures. Energy & Fuels 2018;32:12695-702. 10.1021/acs.energyfuels.8b02750
[122] Lei Z, Dai C, Chen B. Gas Solubility in Ionic Liquids. Chemical Reviews 2014;114:1289-326. 10.1021/cr300497a
[123] Harris KR, Kanakubo M. High pressure studies of the transport properties of ionic liquids. Faraday Discussions 2012;154:425-38. 10.1039/C1FD00085C
[124] Zhang W, Ye L, Jiang J. CO2 capture with complex absorbent of ionic liquid, surfactant and water. Journal of Environmental Chemical Engineering 2015;3:227-32. https://doi.org/10.1016/j.jece.2014.07.020
[125] Anderson JL, Dixon JK, Brennecke JF. Solubility of CO2, CH4, C2H6, C2H4, O2, and N2 in 1-Hexyl-3-methylpyridinium Bis(trifluoromethylsulfonyl)imide: Comparison to Other Ionic Liquids. Accounts of Chemical Research 2007;40:1208-16. 10.1021/ar7001649
[126] Li X, Zhang L, Zheng Y, Zheng C. Effect of SO2 on CO2 Absorption in Flue Gas by Ionic Liquid 1-Ethyl-3-methylimidazolium Acetate. Industrial & Engineering Chemistry Research 2015;54:8569-78. 10.1021/acs.iecr.5b02208
[127] McKone JR, Lewis NS, Gray HB. Will Solar-Driven Water-Splitting Devices See the Light of Day? Chemistry of Materials 2014;26:407-14. 10.1021/cm4021518
[128] Sacco A, Speranza R, Savino U, Zeng J, Farkhondehfal MA, Lamberti A, et al. An Integrated Device for the Solar-Driven Electrochemical Conversion of CO2 to CO. ACS Sustainable Chemistry & Engineering 2020;8:7563-8. 10.1021/acssuschemeng.0c02088
[129] Wenham SR, Green MA. Silicon solar cells. Progress in Photovoltaics: Research and Applications 1996;4:3-33. https://doi.org/10.1002/(SICI)1099-159X(199601/02)4:1<3::AID-PIP117>3.0.CO;2-S
[130] Bagnall DM, Boreland M. Photovoltaic technologies. Energy Policy 2008;36:4390-6. https://doi.org/10.1016/j.enpol.2008.09.070
[131] Lee TD, Ebong AU. A review of thin film solar cell technologies and challenges. Renewable and Sustainable Energy Reviews 2017;70:1286-97. https://doi.org/10.1016/j.rser.2016.12.028
[132] Gong J, Sumathy K, Qiao Q, Zhou Z. Review on dye-sensitized solar cells (DSSCs): Advanced techniques and research trends. Renewable and Sustainable Energy Reviews 2017;68:234-46. https://doi.org/10.1016/j.rser.2016.09.097
[133] Shalini S, Balasundaraprabhu R, Kumar TS, Prabavathy N, Senthilarasu S, Prasanna S. Status and outlook of sensitizers/dyes used in dye sensitized solar cells (DSSC): a review. International Journal of Energy Research 2016;40:1303-20. https://doi.org/10.1002/er.3538
[134] Shakeel Ahmad M, Pandey AK, Abd Rahim N. Advancements in the development of TiO2 photoanodes and its fabrication methods for dye sensitized solar cell (DSSC) applications. A review. Renewable and Sustainable Energy Reviews 2017;77:89-108. https://doi.org/10.1016/j.rser.2017.03.129
[135] Park N-G. Perovskite solar cells: an emerging photovoltaic technology. Materials Today 2015;18:65-72. https://doi.org/10.1016/j.mattod.2014.07.007
[136] Green MA, Ho-Baillie A, Snaith HJ. The emergence of perovskite solar cells. Nature Photonics 2014;8:506-14. 10.1038/nphoton.2014.134
[137] Yu W, Sun X, Xiao M, Hou T, Liu X, Zheng B, et al. Recent advances on interface engineering of perovskite solar cells. Nano Research 2022;15:85-103. 10.1007/s12274-021-3488-7
[138] Winkler MT, Cox CR, Nocera DG, Buonassisi T. Modeling integrated photovoltaic–electrochemical devices using steady-state equivalent circuits. Proceedings of the National Academy of Sciences 2013;110:E1076-E82. doi:10.1073/pnas.1301532110
[139] Gurudayal, Bullock J, Srankó DF, Towle CM, Lum Y, Hettick M, et al. Efficient solar-driven electrochemical CO2 reduction to hydrocarbons and oxygenates. Energy & Environmental Science 2017;10:2222-30. 10.1039/C7EE01764B

[140] Schreier M, Curvat L, Giordano F, Steier L, Abate A, Zakeeruddin SM, et al. Efficient photosynthesis of carbon monoxide from CO2 using perovskite photovoltaics. Nature Communications 2015;6:7326. 10.1038/ncomms8326
[141] Arai T, Sato S, Sekizawa K, Suzuki TM, Morikawa T. Solar-driven CO2 to CO reduction utilizing H2O as an electron donor by earth-abundant Mn-bipyridine complex and Ni-modified Fe-oxyhydroxide catalysts activated in a single-compartment reactor. Chemical Communications 2019;55:237-40. 10.1039/c8cc07900e
[142] Nishi T, Sato S, Sekizawa K, Suzuki TM, Oh-ishi K, Takahashi N, et al. Carbon Nanohorn Support for Solar driven CO2 Reduction to CO Catalyzed by Mn-complex in an All Earth-abundant System. ChemNanoMat 2021;7:596-9. 10.1002/cnma.202100081
[143] Schreier M, Héroguel F, Steier L, Ahmad S, Luterbacher JS, Mayer MT, et al. Solar conversion of CO2 to CO using Earth-abundant electrocatalysts prepared by atomic layer modification of CuO. Nature Energy 2017;2:17087. 10.1038/nenergy.2017.87
[144] Chung J, Jeon NJ, Noh JH. Solar-Driven Simultaneous Electrochemical CO2 Reduction and Water Oxidation Using Perovskite Solar Cells. Energies 2022;15. 10.3390/en15010270
[145] Bae H, Seong C, Burungale V, Seol M, Yoon CO, Kang SH, et al. Nanostructured Au Electrode with 100 h Stability for Solar-Driven Electrochemical Reduction of Carbon Dioxide to Carbon Monoxide. ACS Omega 2022;7:9422-9. 10.1021/acsomega.1c06720
[146] Zhang W, Xia Y, Chen S, Hu Y, Yang S, Tie Z, et al. Single-Atom Metal Anchored Zr6-Cluster-Porphyrin Framework Hollow Nanocapsules with Ultrahigh Active-Center Density for Electrocatalytic CO2Reduction. Nano Letters 2022;22:3340-8. 10.1021/acs.nanolett.2c00547
[147] Wang Y, Liu J, Wang Y, Wang Y, Zheng G. Efficient solar-driven electrocatalytic CO2 reduction in a redox-medium-assisted system. Nature Communications 2018;9:5003. 10.1038/s41467-018-07380-x
[148] Ma W, Wang H, Yu W, Wang X, Xu Z, Zong X, et al. Achieving Simultaneous CO2 and H2S Conversion via a Coupled Solar-Driven Electrochemical Approach on Non-Precious-Metal Catalysts. Angewandte Chemie - International Edition 2018;57:3473-7. 10.1002/anie.201713029
[149] Kim B, Seong H, Song JT, Kwak K, Song H, Tan YC, et al. Over a 15.9% Solar-to-CO Conversion from Dilute CO2 Streams Catalyzed by Gold Nanoclusters Exhibiting a High CO2 Binding Affinity. ACS Energy Letters 2020;5:749-57. 10.1021/acsenergylett.9b02511
[150] Cheng WH, Richter MH, Sullivan I, Larson DM, Xiang C, Brunschwig BS, et al. CO2 Reduction to CO with 19% Efficiency in a Solar-Driven Gas Diffusion Electrode Flow Cell under Outdoor Solar Illumination. ACS Energy Letters 2020:470-6. 10.1021/acsenergylett.9b02576
[151] Wang C, Ren H, Wang Z, Guan Q, Liu Y, Li W. A promising single-atom Co-N-C catalyst for efficient CO2 electroreduction and high-current solar conversion of CO2 to CO. Applied Catalysis B: Environmental 2022;304. 10.1016/j.apcatb.2021.120958
[152] Lee WH, Lim C, Ban E, Bae S, Ko J, Lee HS, et al. W@Ag dendrites as efficient and durable electrocatalyst for solar-to-CO conversion using scalable photovoltaic-electrochemical system. Applied Catalysis B: Environmental 2021;297. 10.1016/j.apcatb.2021.120427